AD 600681

RTD-TDR-63-4022

AERODYNAMIC CHARACTERISTICS OF THE PARAFOIL GLIDER AND OTHER GLIDING PARACHUTES

TECHNICAL DOCUMENTARY REPORT No. RTD-TDR-63-4022

APRIL 1964

AIR FORCE FLIGHT DYNAMICS LABORATORY
RESEARCH AND TECHNOLOGY DIVISION
AIR FORCE SYSTEMS COMMAND
WRIGHT-PATTERSON AIR FORCE BASE, OHIO

Project No. 6065, Task No. 606503

(Prepared under Contract No. AF 33(616)-8310
Department of Aeronautics and Engineering Mechanics,
University of Minnesota, Minneapolis, Minnesota
Authors: H. G. Heinrich, Thomas Nietz, Harvey Lippa)

REPRODUCED BY
NATIONAL TECHNICAL
INFORMATION SERVICE
U.S. DEPARTMENT OF COMMERCE
SPRINGFIELD, VA. 22161

N O T I C E

THIS DOCUMENT HAS BEEN REPRODUCED FROM THE BEST COPY FURNISHED US BY THE SPONSORING AGENCY. ALTHOUGH IT IS RECOGNIZED THAT CERTAIN PORTIONS ARE ILLEGIBLE, IT IS BEING RELEASED IN THE INTEREST OF MAKING AVAILABLE AS MUCH INFORMATION AS POSSIBLE.

FOREWORD

This report was prepared by the staff of the Department of Aeronautics and Engineering Mechanics of the University of Minnesota in compliance with Air Force Contract Number AF 33(616)-8310, Project No 6065, Task No 606503, "Theoretical Parachute Investigations." The work being accomplished under this contract is jointly sponsored by the QM Research and Engineering Command, Department of the Army; Bureau of Aeronautics and Bureau of Ordnance, Department of the Navy; and Air Force Systems Command, Department of the Air Force; and is directed by a Tri-Service Steering Committee concerned with aerodynamic retardation. The contract administration has been conducted by the Research and Technology Division (AFSC), and Messrs. Rudi J. Berndt and James H. DeWeese of the Recovery and Crew Station Branch, Air Force Flight Dynamics Laboratory, Research and Technology Division, have been project engineers.

Messrs. Eugene Haak, Ronald Niccum, W. Richard Mueller, and a number of graduate and undergraduate students of the University of Minnesota have contributed to the reported objective, and the authors wish to express their appreciation to them.

ABSTRACT

A newly conceived gliding parachute, called the parafoil glider, and several existing glide parachutes have been examined with regard to their general stability, resulting stable angle of attack, and lift to drag ratio. The parafoil glider assumed stable angles of attack up to 50° against the vertical which represents a lift to drag ratio of approximately 1.2. The investigated existing parachutes had lift to drag ratios of less than unity. The tangential force coefficient of the parafoil glider amounts to approximately 1.5 at the position of the stable angle of attack.

This technical documentary report has been reviewed and is approved.

Theron J. Baker
Vehicle Equipment Division
Air Force Flight Dynamics Laboratory

Preceding page blank

TABLE OF CONTENTS

Section		Page
I.	Introduction	1
II.	Models	5
	A. Rigid Models	5
	B. Fabric Models	5
III.	Experimental Procedure	20
	A. Gliding Parachute Nomenclature	20
	B. Rigid Model Test Procedure	20
	C. Flexible Model Test Procedure	22
IV.	Analysis and Results	25
	A. Rigid Models	25
	B. Fabric Models	25
	C. Three-Component Tests	28
V.	Summary and Conclusions	33
	Appendix: Design, Development, and Modification of the PARAFOIL GLIDER	34
	References	48

LIST OF ILLUSTRATIONS

Figure No		Page
1.	Forces and Coordinates for Gliding Parachute	1
2.	26-Inch Nominal Diameter Circular Flat Parachute Modified with Extensions ($\alpha = 6° \pm 3°$)	3
3.	70-Inch Nominal Diameter Extended Skirt Canopy with Modified Extensions ($\alpha = 22° \pm 3°$)	3
4.	26-Inch Nominal Diameter T-10 Extended Skirt Parachute with Unsymmetrical Extensions ($\alpha = 12° \pm 3°$)	3
5.	A/P 28S-3 Steerable Parachute Modified From an MC-1 with a Single Orifice ($\alpha = 20° \pm 3°$)	3
6.	a) Extended Skirt Parachute Canopy	6
	b) Extended Skirt Parachute Canopy with Lateral Extensions (Model a)	6
7.	a) Extended Skirt Parachute Canopy	6
	b) Extended Skirt Canopy Modified with Plastelina (Model b)	6
8.	a) Elliptical Cross Section Extended Skirt Canopy	6
	b) Elliptical Extended Skirt Canopy Modified with Plastelina (Model c)	6
9.	Gliding Parachute Modified from 10% Extended Skirt Parachute (Model d)	7
10.	Gliding Parachute Modified from 10% Extended Skirt Parachute (Model e)	7
11.	32-Inch Diameter Unsymmetrical Gliding Parachute in Wind Tunnel (Model 1)	8
12.	Unsymmetrical Parachute Gore Pattern-- 32-Inch Nominal Diameter (Model 1)	8
13.	Schematic Drawing of a Gliding Parachute Modified from a 10% Extended Skirt Canopy (Model 2)	9

LIST OF ILLUSTRATIONS (CONT)

Figure No		Page
14.	Gliding Parachute Modified from a 37.5-Inch Nominal Diameter 10% Extended Skirt Canopy (Model 2)	9
15.	Gliding Parachute Modified From a 10% Extended Skirt Canopy (Model 3)	10
16.	16-Inch Nominal Diameter Gliding Parachute Modified From a 10% Extended Skirt Canopy in Wind Tunnel (Model 3)	10
17.	Gliding Parachute Modified From a 12-Inch Diameter Ribbed Guide Surface Parachute in Wind Tunnel (Model 4)	13
18.	16-Inch Diameter Gliding Parachute Constructed of Zero Porosity Mylar-Coated Nylon (Model 5).	12
19.	24-Inch Diameter Gliding Parachute Constructed of 30 Porosity Nylon Cloth (Model 6)	13
20.	24-Inch Diameter Parafoil Glider Constructed of 10 Porosity Nylon (Model 7)	15
21.	Schematic Drawing of Basic Plans Used in Constructing the Parafoil Glider, Models 7, 8, and 9	16
22.	10-Ft Diameter Parafoil Glider Constructed of 10 Porosity Nylon Cloth (Model 8)	17
23.	16-Inch Diameter Parafoil Glider Used for Three-Component Studies of Models in Figs 21 and 23; Made of 10 Porosity Nylon Cloth (Model 9)	18
24.	36-Inch Diameter Parafoil Glider Made of 10 Porosity Nylon Cloth With 32 Suspension Lines (Model 10)	19
25.	Stability Notation for Gliding Parachute . . .	21
26.	Wind Tunnel Test Arrangement	22
27.	Subsonic Wind Tunnel Test Arrangement	23
28.	Angular Deflection Indicator	23

LIST OF ILLUSTRATIONS (CONT)

Figure No		Page
29.	Characteristic Coefficients Vs. Angle of Attack for Model 3, a Gliding Parachute Modified from a 10% Extended Skirt Canopy (Based on Total Surface Area, S_o, and Reynolds Number = 5.6 x 10^5)	29
30.	Characteristic Coefficients Vs. Angle of Attack for Model 5, a Gliding Parachute Constructed With Zero Porosity Mylar-Coated Nylon (Based on Total Surface Area, S_o, and Reynolds Number = 5.6 x 10^5)	30
31.	Characteristic Coefficients Vs. Angle of Attack for a Parafoil Glider Constructed With 10 Porosity Nylon at Various Line Adjustments (Based on Total Surface Area, S_o, and Reynolds Number = 5.0 x 10^5)	31
32.	Profile Views of 24-Suspension Line Parafoil Glider	36
33.	Inflated Parachute Canopy in Wind Tunnel (24-Suspension Line Model)	37
34.	Schematic View of Individual Gores	38
35.	Dimensionless Pattern for Gore No. 1	39
36.	Dimensionless Pattern for Gore No. 2	40
37.	Dimensionless Pattern for Gore No. 3	41
38.	Dimensionless Pattern for Gore No. 4	42
39.	Dimensionless Pattern for Gore No. 5	43
40.	Suspension Line Length for 24-Suspension Line Parafoil Glider	44
41.	Typical Rib Profile of the Parafoil Glider . .	45
42.	Top View of Inflated Canopy Planform and Rib Locations	45
43.	Dimensionless Gore Patterns for Front Ribs of Parafoil Glider	47
44.	Dimensionless Gore Patterns for Rear Ribs of Parafoil Glider	47

LIST OF TABLES

Table No		Page
1.	Summary of Results for Rigid Parachute Models	26
2.	Tabulated Results for Fabric Parachute Models	27

LIST OF SYMBOLS

α	=	angle of attack (degrees)
C_N	=	normal force coefficient
C_M	=	pitching moment coefficient ("moment coefficient")
C_T	=	tangent force coefficient
D	=	drag
D_o	=	nominal diameter $= \sqrt{\frac{4S_o}{\pi}}$
L	=	lift
L_T	=	length of trailing edge suspension lines
L_l	=	length of leading edge suspension lines
M	=	pitching moment ("moment")
N	=	normal force
S_o	=	canopy surface area
T	=	tangent force
V	=	velocity (ft/sec)

I. INTRODUCTION

With most conventional parachutes, the stable angle of attack is such that the parachute develops lift as well as drag. When this occurs the parachute is said to "glide" or to fly at an angle of attack; the angle of attack, α, is determined by the ratio of the lift and drag forces, L/D, and it can be seen from Fig 1 that $\alpha = \tan^{-1} L/D$.

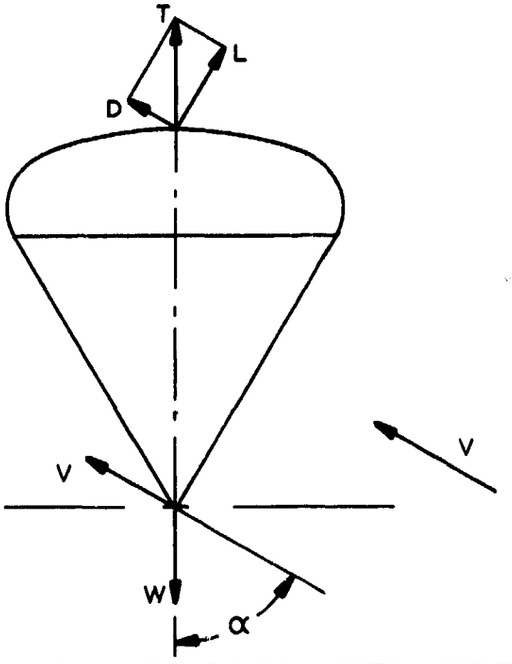

FIG 1. FORCES AND COORDINATES FOR GLIDING PARACHUTE

When gliding, the aerodynamic forces of the parachute and the suspended weight are in equilibrium. In order to maintain the position of equilibrium, the forces acting on the canopy at other than the stable angle of attack must be such that they develop a restoring moment toward the stable position.

It is the objective of this study to develop a self-inflating aerodynamic decelerator with a high lift to drag ratio, possibly of two (2). For a lift to drag ratio of 2,

Manuscript released by the authors December, 1962, for publication as an RTD Technical Documentary Report.

the angle of attack of the parachute would be $\alpha_{stable} = 63.5°$. Thus this parachute would glide during its descent at an angle of 26.5° relative to the horizon.

A first step in this investigation was to test the following four (4) existing unsymmetrical parachutes in the subsonic wind tunnel at the University of Minnesota and in low level drop tests:

a) A 26-inch nominal diameter circular flat canopy with two double-sized slanted and ten straight personnel guide surface-type extensions (see Fig 2). This parachute was found to have a stable angle of attack of 6° ± 3° corresponding to an L/D of 0.11.

b) A 70-inch nominal diameter extended skirt canopy modified with diametrically opposite, slanted and vented guide surface extensions as shown in Fig 3. This model achieved a stable angle of attack of 22° ± 3°, corresponding to an L/D of 0.40.

c) A 26-inch nominal diameter T-10 extended skirt canopy modified with an unsymmetrical arrangement of personnel guide surface type of extensions as shown in Fig 4. This configuration has a stable angle of attack of 12° ± 3°, corresponding to an L/D of 0.21.

d) An A/P28S-3 steerable parachute modified from a 37.5 inch nominal diameter MC-1 canopy with a single orifice as shown in Fig 5. It was found that this parachute had a stable angle of attack of 20° ± 3°, corresponding to an L/D of 0.36.

None of these parachutes approaches the desired L/D ratio of 2. There are more gliding parachutes, however, such as the "Blanc Gore" or the "Sky Sail" parachute. However, it is known that these types also glide at about 20 to 25 degrees against the vertical (Ref 3). Therefore, it was decided to initiate a more basic study with unconventional forms. This resulted in a new parachute configuration of solid cloth

FIG 2. 26-IN. NOMINAL DIAMETER CIRCULAR FLAT PARACHUTE MODIFIED WITH EXTENSIONS $\alpha = 6° \pm 3°$

FIG 3. 70-IN. NOMINAL DIAMETER EXTENDED SKIRT CANOPY WITH MODIFIED EXTENSIONS $\alpha = 22° \pm 3°$

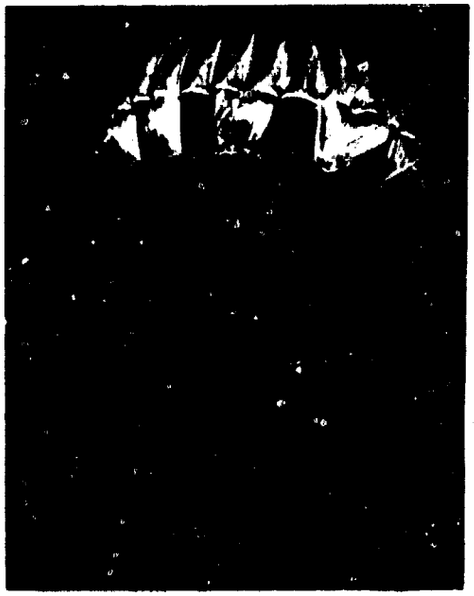

FIG 4. 26-IN. NOMINAL DIAMETER T-10 EXTENDED SKIRT PARACHUTE WITH UNSYMETRICAL EXTENSIONS $\alpha = 12° \pm 3°$

FIG 5. A/P 28S-3 STEERABLE PARACHUTE MODIFIED FROM MC-1 CANOPY WITH A SINGLE ORIFICE $\alpha = 20° \pm 3°$

called PARAFOIL GLIDER, which achieved glide angles up to 50° against the vertical which is equivalent to a lift to drag ratio of 1.2.

II. MODELS

A. Rigid Models

Eight rigid models have been tested in the open section of the wind tunnel. These models were used as an initial investigation in search of a parachute which would have an L/D of 2. The models are:

a) an extended skirt canopy with two lateral extensions constructed of balsa wood and Plastelina (Fig 6),

b) an extended skirt canopy modified with a stabilizing downstream extension (Figs 7a,b),

c) an elliptical canopy with two gliding surfaces at the downstream part (Figs 8a,b),

d) an extended skirt canopy with a single gliding surface (Fig 9), and

e) an extended skirt canopy with gliding surface and exhaust jet in rear of the canopy (Fig 10).

B. Fabric Models

In addition to the tests with rigid models, many experiments were conducted with gliding parachutes made out of nylon cloth. These models ranged in size from a 16" nominal diameter, used for three-component measurements, to a 10' nominal diameter for drop testing. These models may be described as follows:

Model 1) A 32-inch nominal diameter unsymmetrical parachute constructed of nylon cloth with a porosity of 120 ft^3/ft^2-min. This configuration is shown in the wind tunnel in Fig 11 and schematically in Fig 12.

Model 2) A gliding parachute modified from a 37.5 inch nominal diameter 10% extended skirt canopy is shown schematically in Fig 13 and in the wind tunnel in Fig 14. This model was constructed of nylon cloth with a porosity of 120 ft^3/ft^2-min and was modeled after rigid model number d.

Model 3) A gliding parachute modified from Model 2. This model is shown schematically in Fig 15 and inflated in Fig 16. It has a nominal diameter of 16 inches

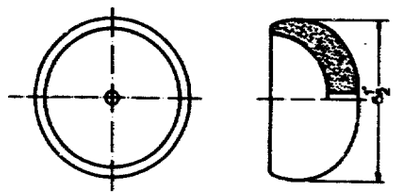

FIG 6a. EXTENDED SKIRT PARACHUTE CANOPY

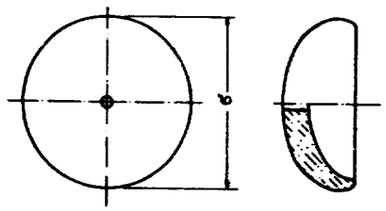

FIG 7a. EXTENDED SKIRT PARACHUTE CANOPY

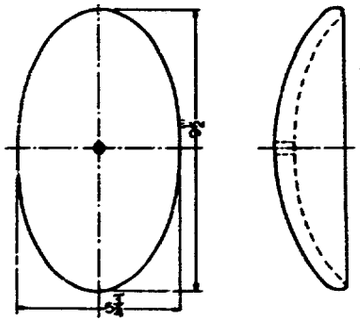

FIG 8a. ELLIPTICAL CROSS SECTION EXTENDED SKIRT CANOPY

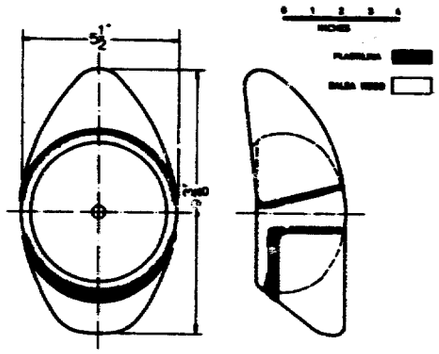

FIG 6b. EXTENDED SKIRT PARACHUTE CANOPY WITH LATERAL EXTENSIONS (Model a)

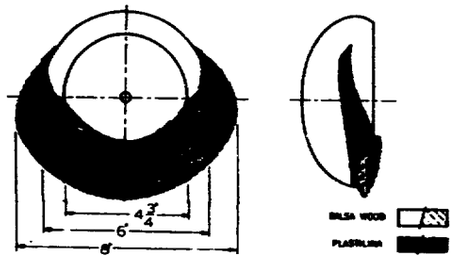

FIG 7b. EXTENDED SKIRT CANOPY MODIFIED WITH PLASTELINA (Model b)

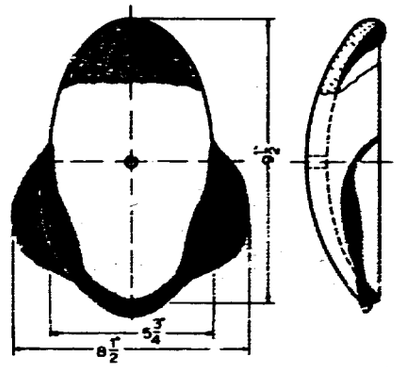

FIG 8b. ELLIPTICAL EXTENDED SKIRT CANOPY MODIFIED WITH PLASTELIMA (Model c)

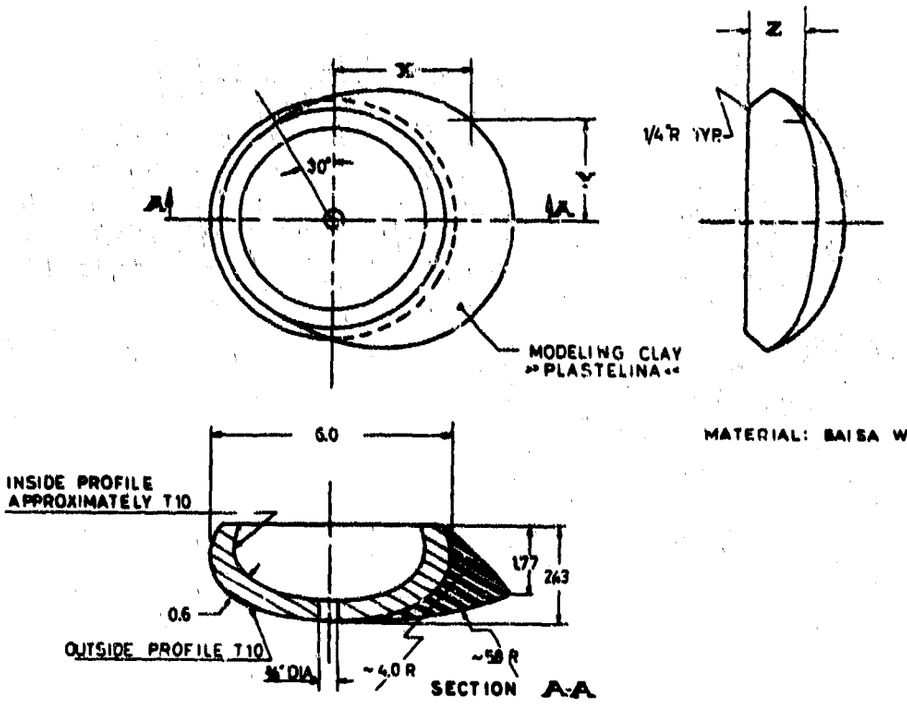

X	Y	Z
0.00	3.20	0.32
1.12	3.32	0.60
1.48	3.33	0.61
2.44	3.14	1.10
3.48	2.58	1.44
4.06	1.94	1.66
4.46	1.00	1.80
4.60	0.00	1.82

FIG 9 GLIDING PARACHUTE MODIFIED FROM 10% EXTENDED SKIRT PARACHUTE (MODEL d)

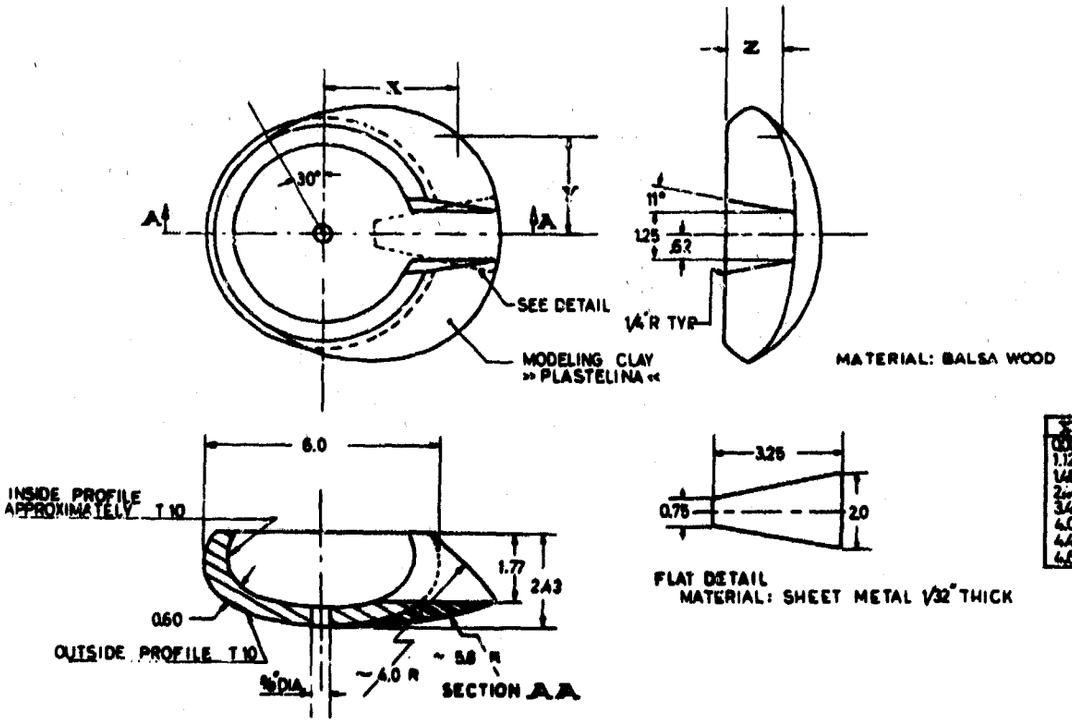

X	Y	Z
0.00	3.20	0.32
1.12	3.32	0.60
1.48	3.33	0.61
2.44	3.14	1.10
3.48	2.58	1.44
4.06	1.94	1.66
4.46	1.00	1.80
4.60	0.00	1.82

FIG 10. GLIDING PARACHUTE MODIFIED FROM 10% EXTENDED SKIRT PARACHUTE (MODEL e.)

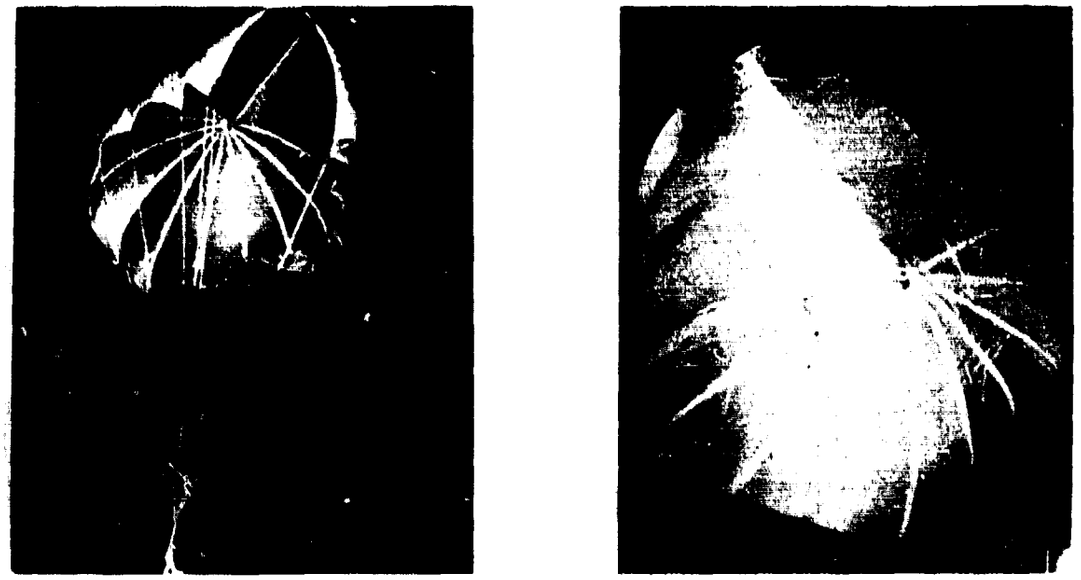

FIG 11. 32-IN. DIAMETER UNSYMETRICAL GLIDING PARACHUTE IN WIND TUNNEL (MODEL 1)

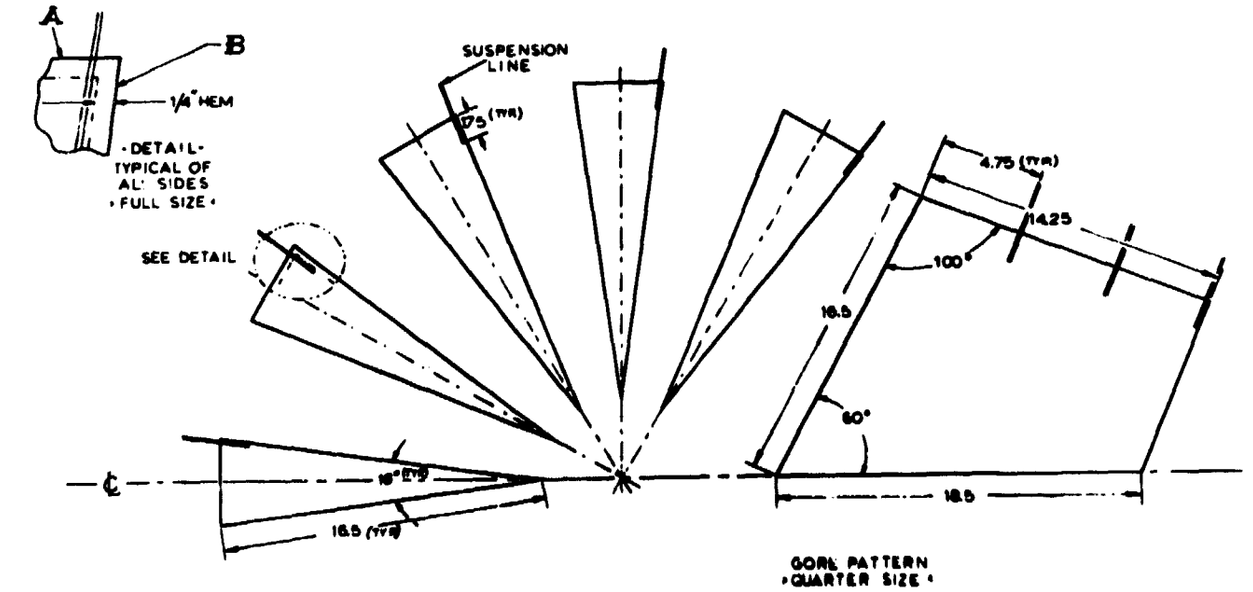

FIG 12. UNSYMMETRICAL PARACHUTE GORE PATTERN — 32-INCH NOMINAL DIAMETER (MODEL 1)

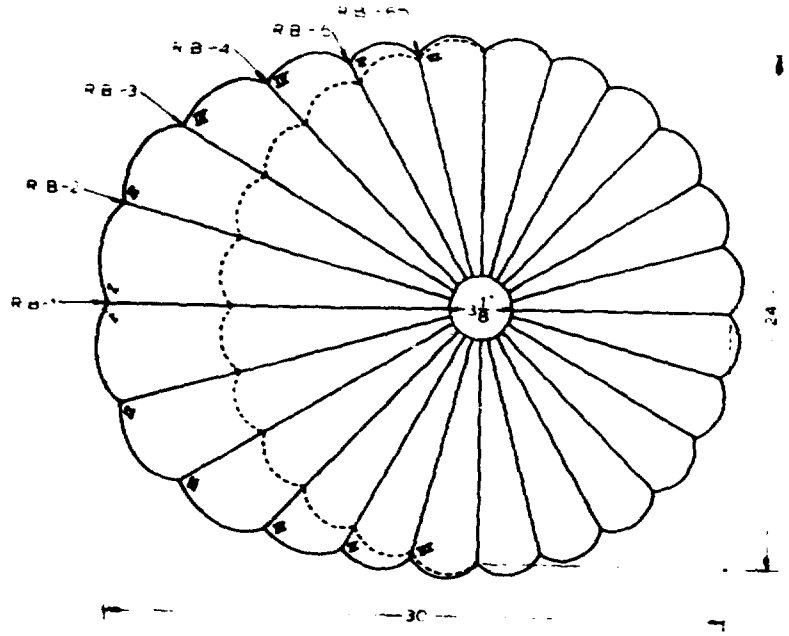

FIG 13. GLIDING PARACHUTE MODIFIED FROM A 10% EXTENDED SKIRT CANOPY (Model 2)

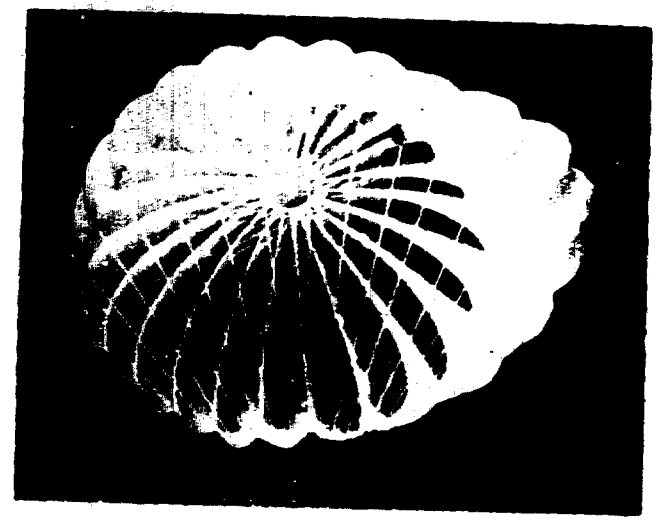

FIG 14. GLIDING PARACHUTE MODIFIED FROM A 37.5-IN. NOMINAL DIAMETER 10% EXTENDED SKIRT CANOPY (MODEL 2)

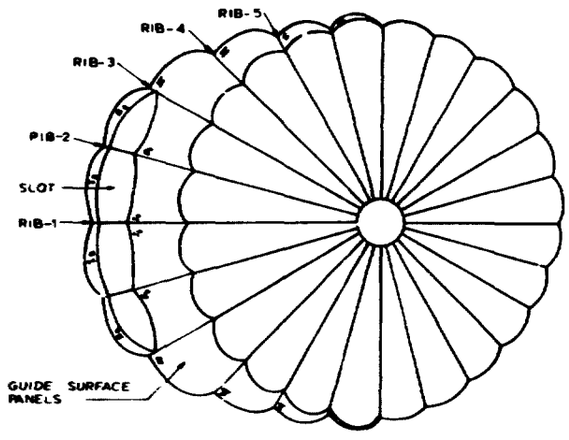

BOTTOM VIEW

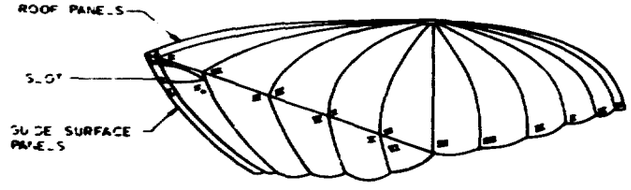

SIDE VIEW

FIG 15. GLIDING PARACHUTE MODIFIED FROM A 10 % EXTENDED SKIRT CANOPY (MODEL 3)

FIG 16. 16 INCH NOMINAL DIAMETER GLIDING PARACHUTE MODIFIED FROM 10 % EXTENDED SKIRT CANOPY IN WIND TUNNEL (MODEL 3)

and is constructed of nylon cloth with a porosity of 120 ft^3/ft^2-min.

The modifications consisted of removing a strip of cloth from the base of eight of the gores contained in the 10 per cent extended skirt portion of the canopy. In addition, slots were cut from four of the guide surface panels along the line of intersection of the roof and guide surface panels. Deflection tests of this model in the open test section of the wind tunnel indicated a maximum stable angle of attack of 35° ± 3°. However, analysis of three-component tests on a smaller model showed the stable angle of attack to be 22° ± 3° (See Table 2). This model was also examined with a zero porosity canopy in which condition a stable angle of attack of 40° ± 3° was achieved.

Another version of this type of parachute was equipped with a large exhaust slot, somewhat similar to Model e, Fig 10. However, the textile model of this version displayed unsatisfactory inflation. Further work on this version was discontinued.

Model 4) A modified 12-inch nominal diameter ribbed guide surface parachute as shown in Fig 17*. This model was constructed from nylon cloth with a porosity of 30 ft^3/ft^2-min. (See Fig 17, on page 13.)

Model 5) A 16-inch nominal diameter gliding parachute constructed with zero porosity mylar-coated nylon as shown in Fig 18*. This model employs the use of longitudinal ribs to support the canopy roof.

*The evolution of Models 4, 5, 6, and 7 is described in the Appendix.

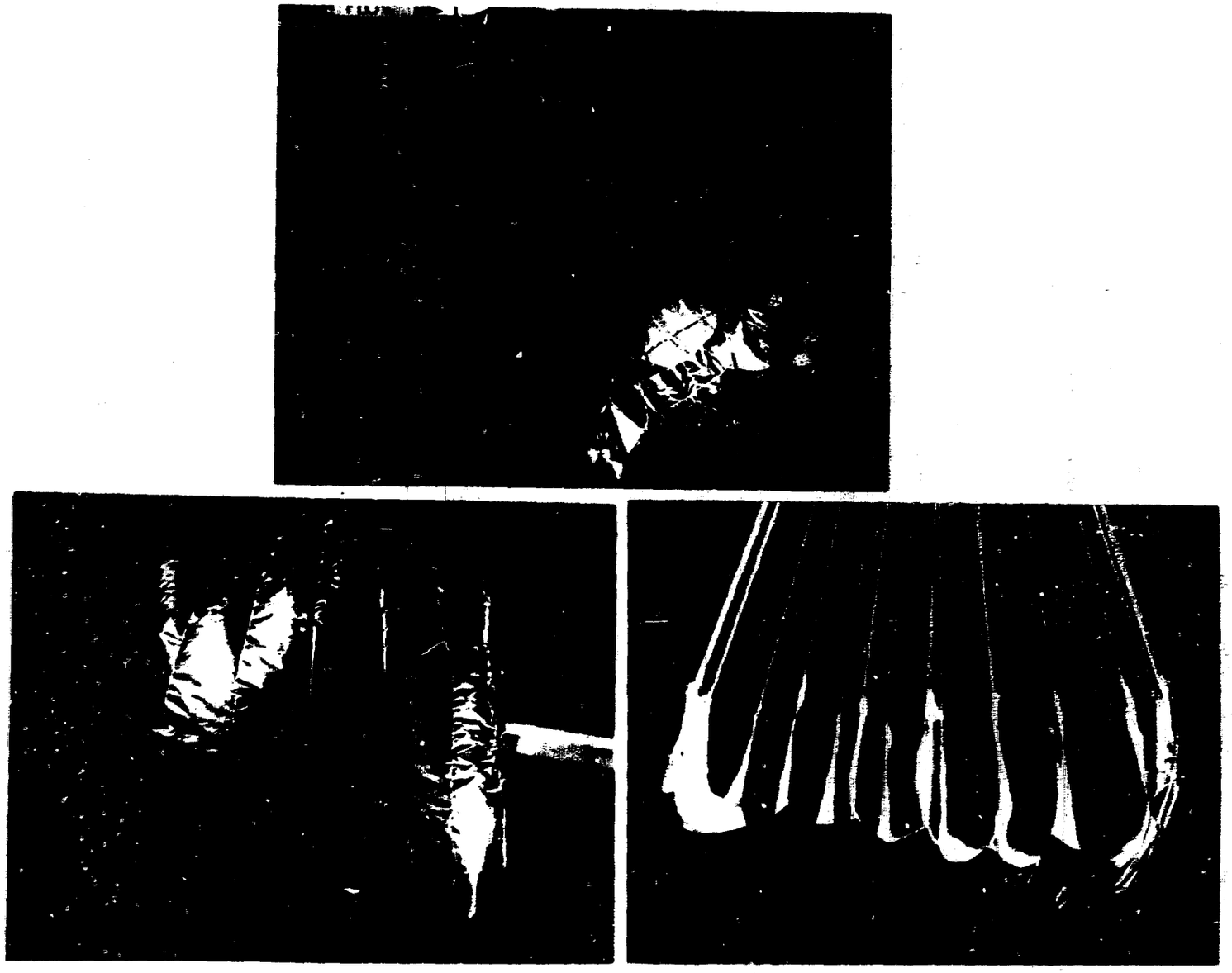

FIG 18. 16-INCH DIAMETER GLIDING PARACHUTE CONSTRUCTED OF ZERO POROSITY MYLAR-COATED NYLON (MODEL 5)

FIG 17. GLIDING PARACHUTE MODIFIED FROM 12 INCH DIAMETER RIBBED GUIDE SURFACE PARACHUTE IN WIND TUNNEL (MODEL 4)

Model 6) A 24-inch nominal diameter parachute of the same design as Model 5 but constructed of nylon cloth with a porosity of 30 ft^3/ft^2-min. This model is shown in Fig 19*. Longitudinal ribs also support the canopy roof.

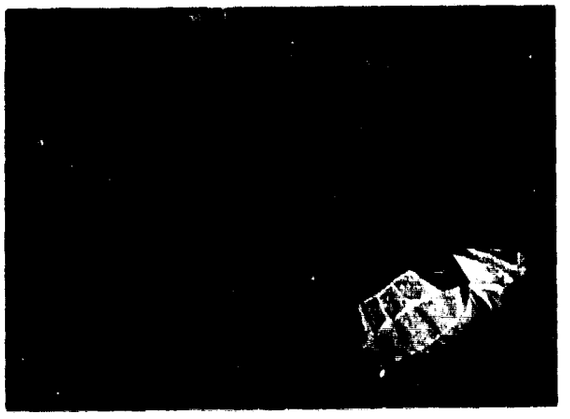

FIG 19. 24 INCH DIAMETER GLIDING PARACHUTE CONTRUCTED FROM 30 POROSITY NYLON CLOTH (MODEL 6)

*The evolution of Models 4, 5, 6, and 7 is described the Appendix

Model 7) A 24-inch nominal diameter parachute constructed from nylon cloth with a porosity of 10 ft^3/ft^2-min. as shown in Fig 20*. This configuration is a variation of Models 5 and 6. The basic design for this canopy is shown schematically in Fig 21 and is the design used in Models 7, 8, 9, and 10. It incorporates all characteristics which, on the basis of this study, are feasible and practical. The configurations 7 through 10 shall, for the purpose of distinction, be called the PARAFOIL GLIDER.

Model 8) A 10-ft nominal diameter replica of Model 7 as shown in Fig 22. This model was constructed from nylon cloth with a porosity of 10 ft^3/ft^2-min.

Model 9) A 16-inch nominal diameter replica of Model 7 as shown in Fig 23. This model was constructed from 10 porosity nylon for use in three component studies.

Model 10) A 36-inch diameter parachute shown in Fig 24 was modeled after the configuration shown in Fig 21. This model was constructed from nylon cloth with a nominal porosity of approximately 10 and has 32 suspension lines.

*The evolution of Models 4, 5, 6, and 7 is described in the Appendix.

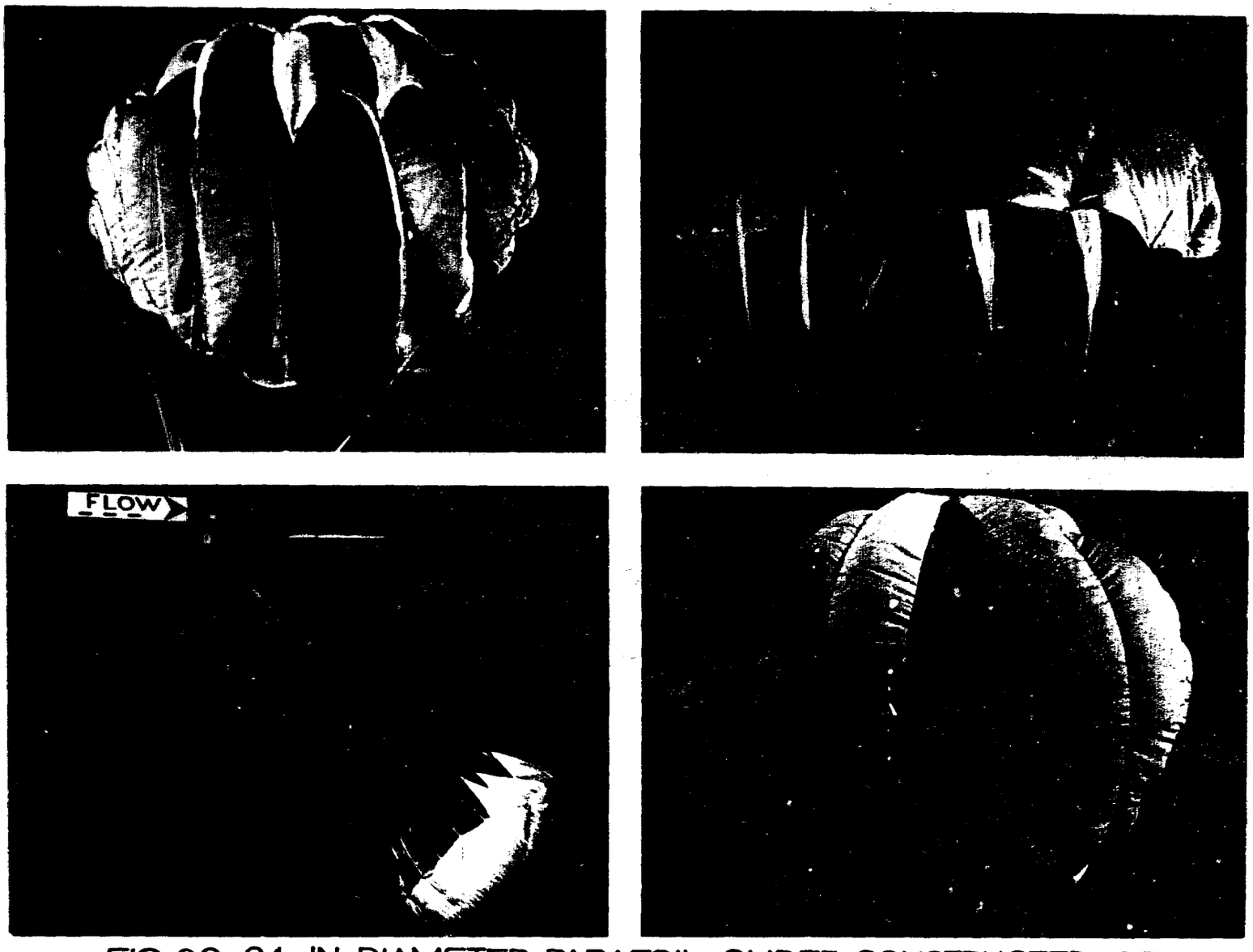

FIG 20 24–IN. DIAMETER PARAFOIL GLIDER CONSTRUCTED OF 10 POROSITY NYLON (MODEL 7)

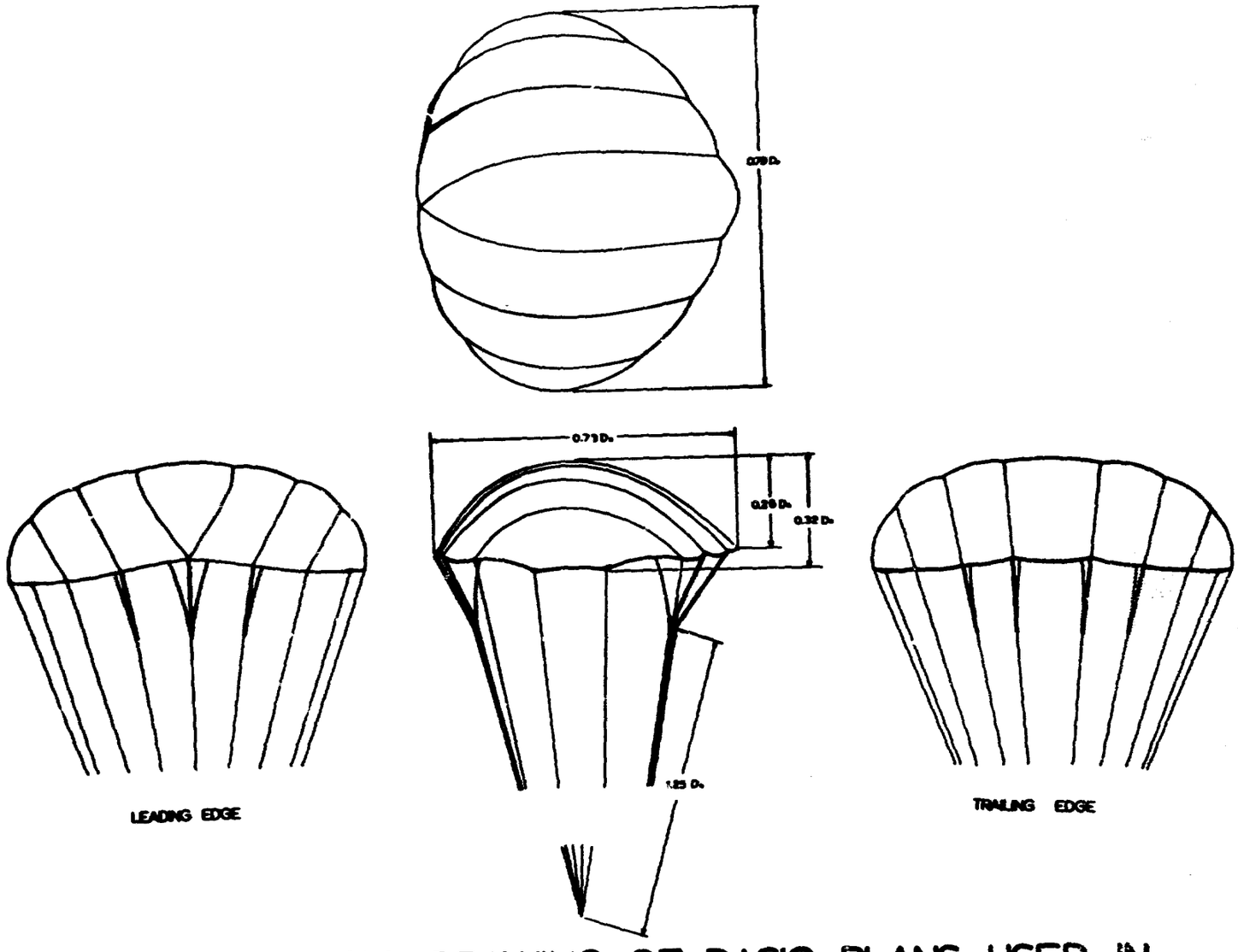

FIG 21. SCHEMATIC DRAWING OF BASIC PLANS USED IN CONSTRUCTING PARAFOIL GLIDER, MODELS 7, 8, AND 9

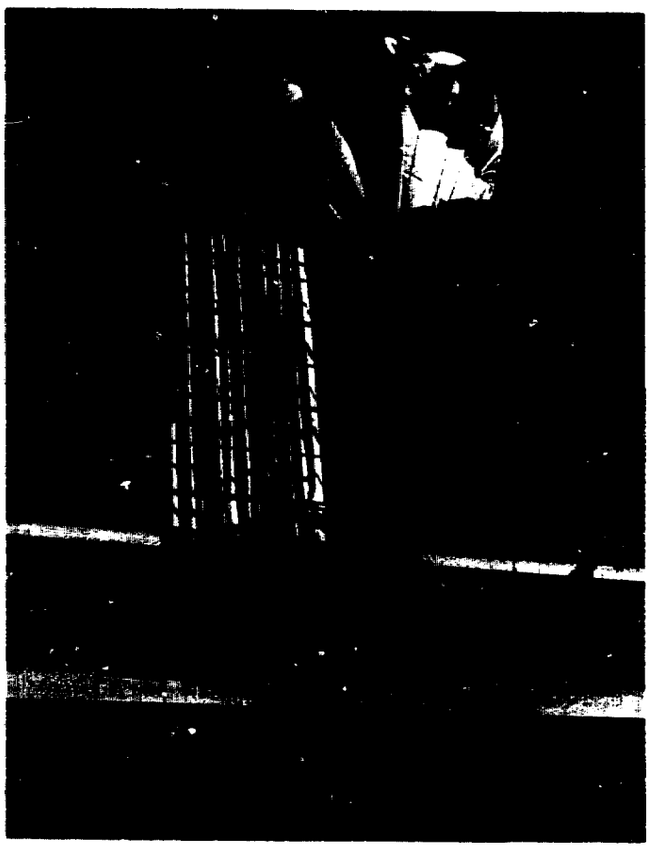

FIG 22. 10-FT. DIAMETER PARAFOIL GLIDER CONSTRUCTED OF 10 POROSITY NYLON CLOTH (MODEL 8)

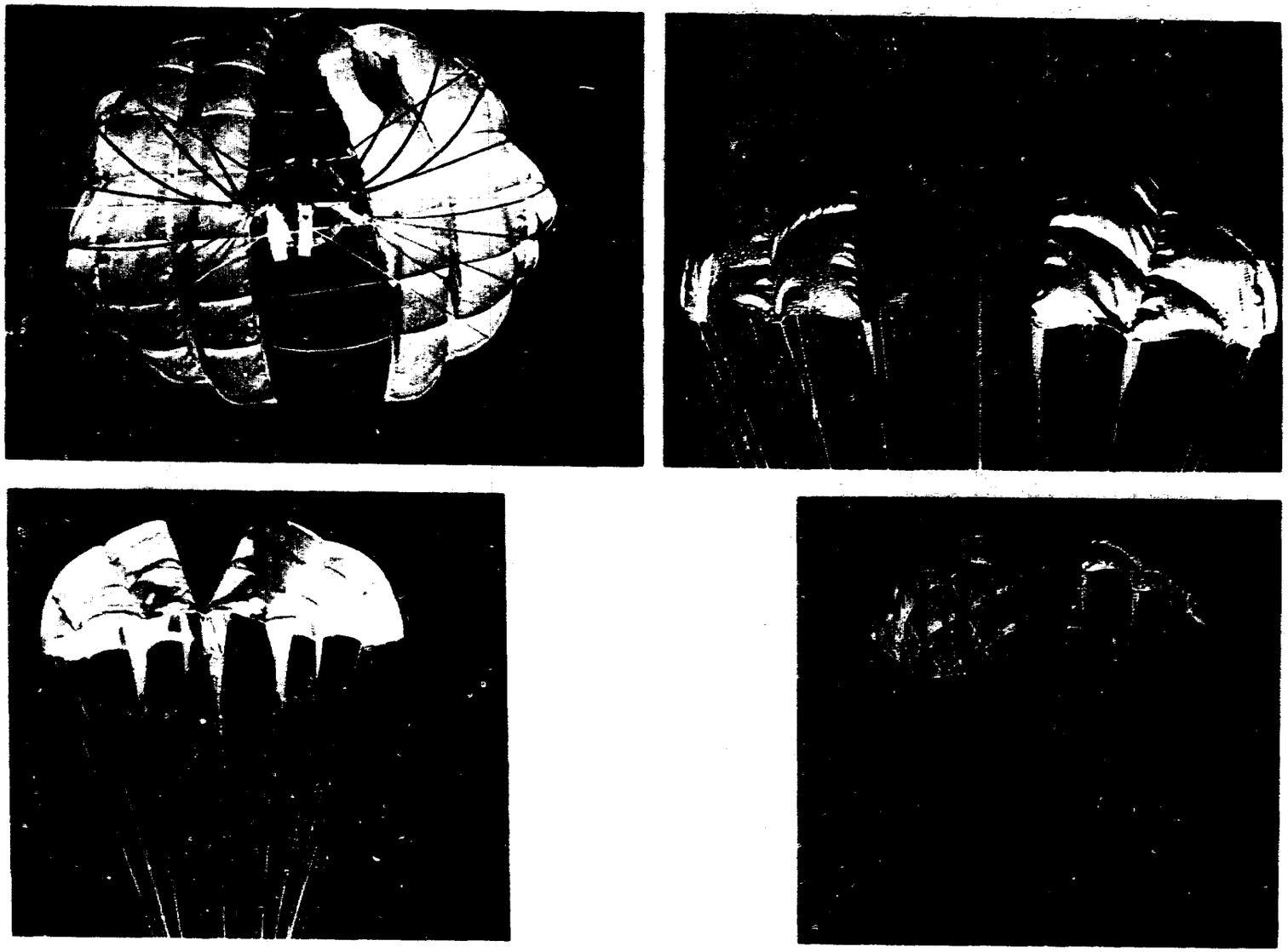

FIG 23. 16-INCH DIAMETER PARAFOIL GLIDER USED FOR THREE-COMPONENT STUDIES OF MODELS IN FIGS. 21 AND 22; MADE OF 10 POROSITY NYLON CLOTH (MODEL 9)

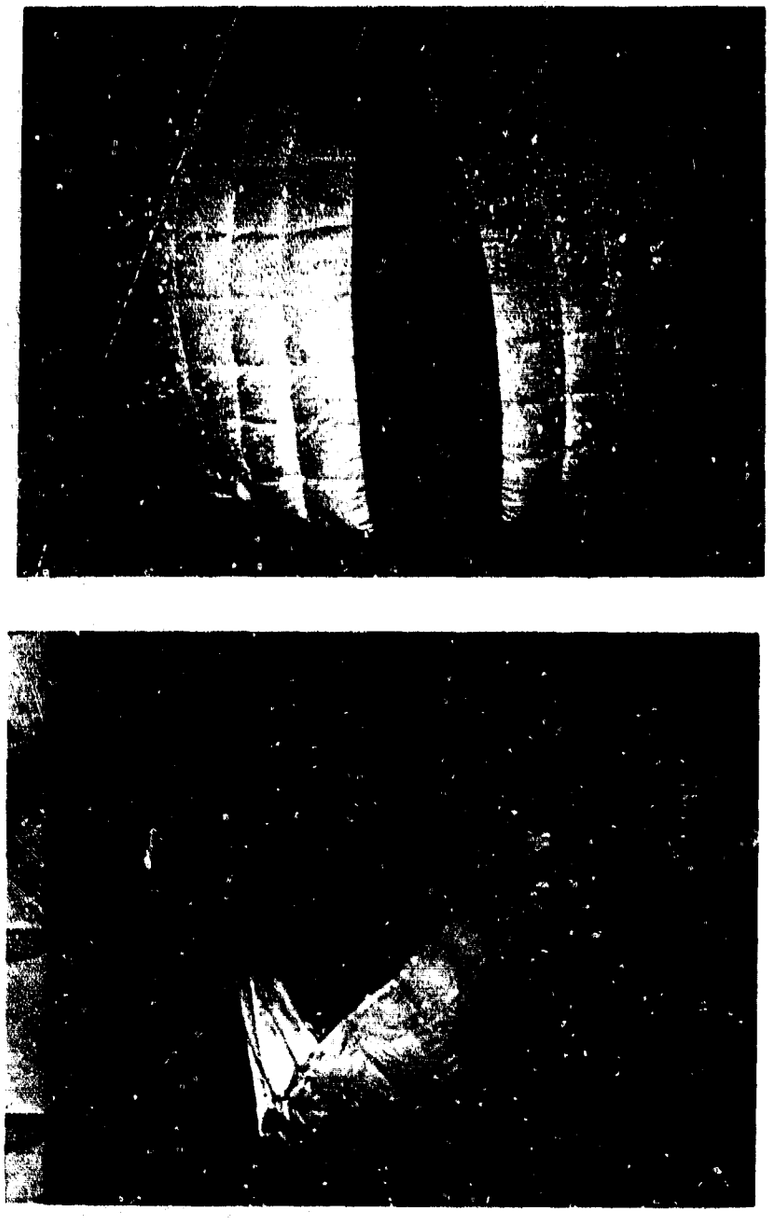

FIG 24. 36-IN. DIAMETER PARAFOIL GLIDER MADE OF 10 POROSITY NYLON CLOTH WITH 32 SUSPENSION LINES (MODEL 10)

III. EXPERIMENTAL PROCEDURE

A. Gliding Parachute Nomenclature

In the course of developing a gliding parachute, it has become convenient to adopt a system of co-ordinates and stability notation. The co-ordinates shown in Fig 25 are a combination of standard parachute and aircraft co-ordinates. This arrangement allows a description of a gliding parachute's performance, which includes the stable angle of attack, α, longitudinal stability, pitch, lateral stability, roll, and yaw stability. Pitch, roll, and yaw are expressed as an angular deviation from the mean stable position. Thus a parachute which has a small angular deviation from its mean, or average position, would be termed a stable configuration.

B. Rigid Model Test Procedure

To expedite the experimental analysis of various parachute configurations, a system has been devised which utilizes rigid models. Rigid models used were fabricated from wood, metal, and Plastelina (a form of modeling clay), or a combination of these materials. This method of testing was previously used in connection with rigid models of conventional parachutes and has been redesigned to accommodate the present testing of gliding parachutes.

The rigid models are mounted on a sting support which is attached to a pivotal device. This pivot restrains the model and sting to movement in a horizontal plane only. A schematic representation of this system is shown in Fig 26.

Experiments performed with rigid models were conducted in the open section of the subsonic wind tunnel at a velocity of approximately 40 ft/sec. For a 6-inch diameter model this velocity yields a Reynolds number on the order of 2×10^5. When the models assume their stable position in the flow, the angle of attack can be read directly from a deflection indicator.

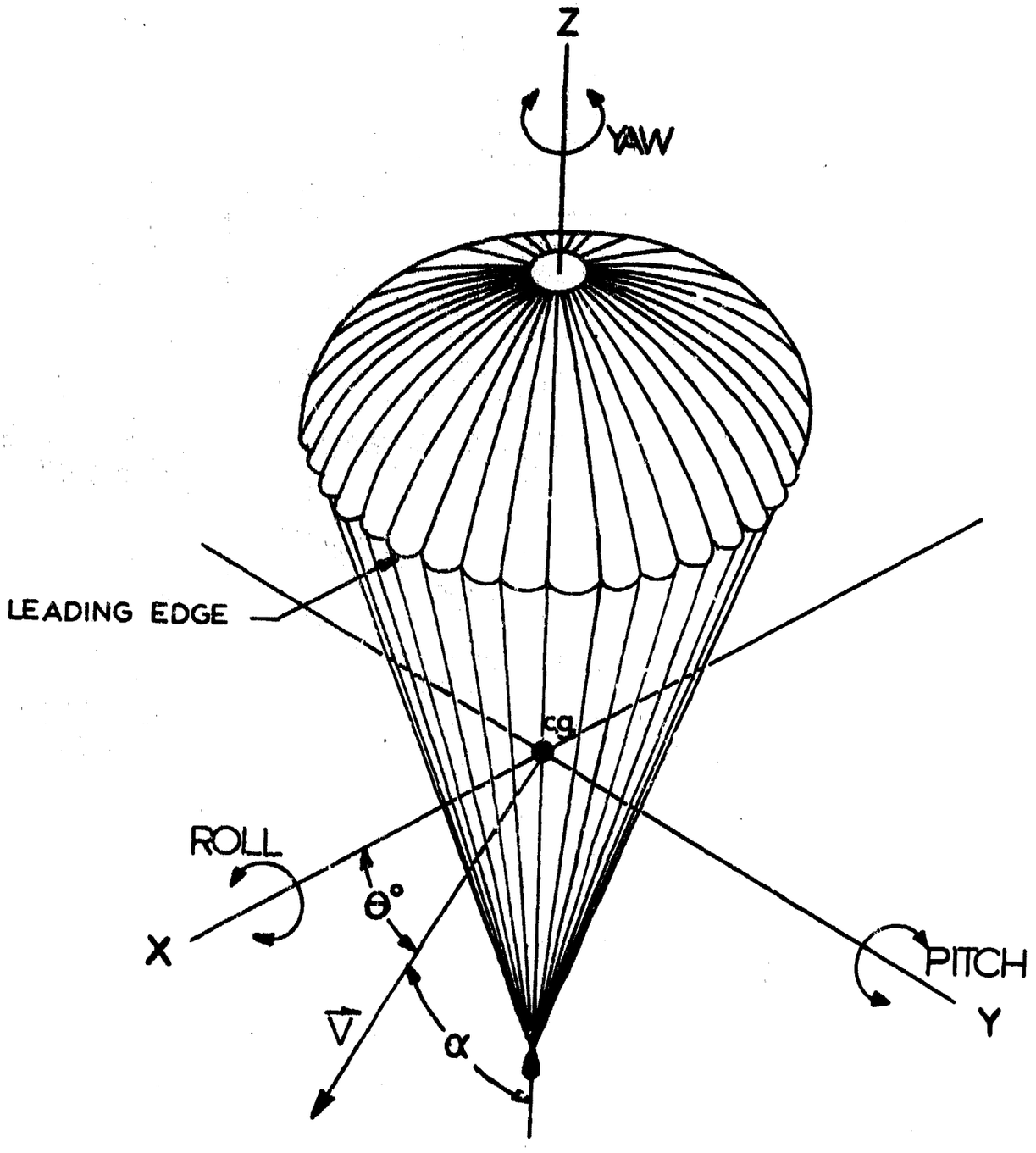

FIG 25. STABILITY NOTATION FOR GLIDING PARACHUTE

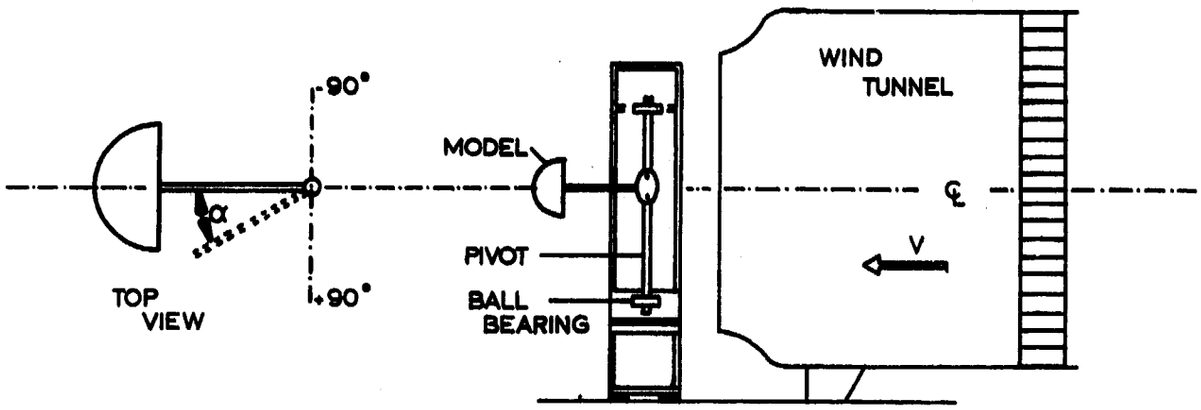

FIG 26. WIND TUNNEL TEST ARRANGEMENT

C. Flexible Model Test Procedure

1) Pendulum Testing Procedure

Experiments with fabric models were conducted in the open section of the wind tunnel at a velocity of approximately 25 ft/sec. For a 24-inch nominal diameter canopy this velocity corresponds to a Reynolds number of approximately 3×10^5.

The models were suspended from a pendulum device which allows free motion in a vertical plane. A schematic representation of the system used is shown in Fig 27 while the pendulum support is shown in Fig 28. The pendulum support is equipped to measure and record the stable angle of attack and the longitudinal stability (pitch) by means of an electrographic recorder while the lateral stability (roll) and the yaw stability are judged by eye.

2) Three Component Measurements

In the advanced stages of development, parachutes are tested in the closed section of the wind tunnel on a three component strain gage balance. The procedure involved for this method of testing is described in Ref 1.

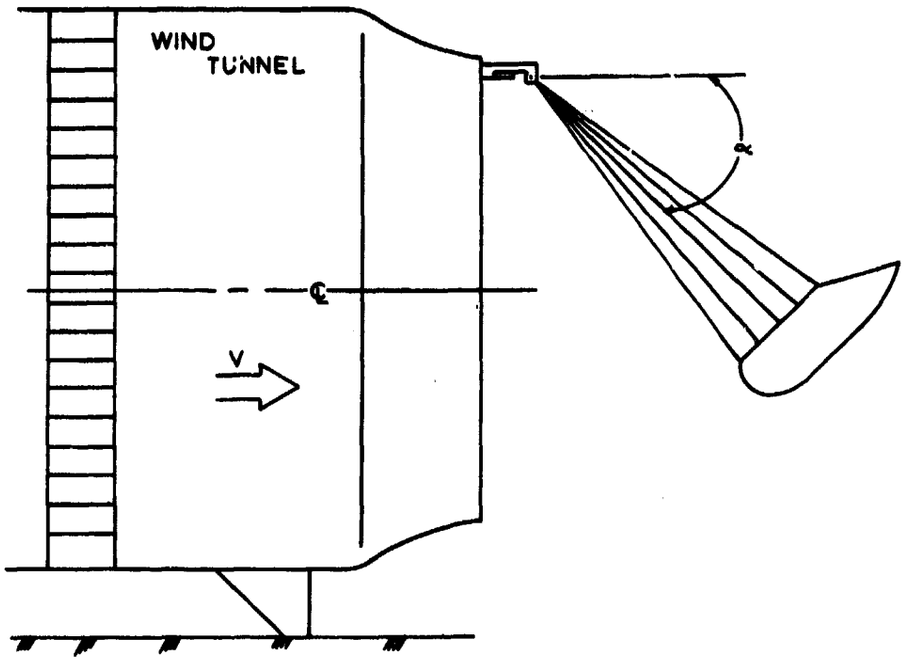

FIG 27. SUBSONIC WIND TUNNEL TEST ARRANGEMENT

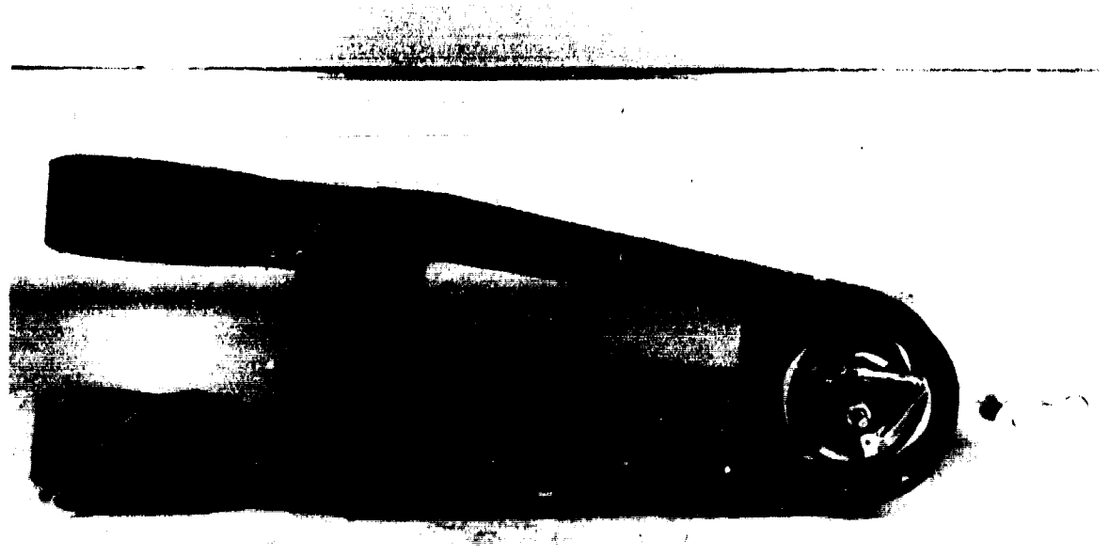

FIG 28. ANGULAR DEFLECTION INDICATOR

The tangent force, T, acts along the centerline of the canopy and is the resultant of the lift and drag as shown in Fig 1. The normal force, N, is perpendicular to the centerline of the canopy and produces the aerodynamic moment, M, about the confluence point of the suspension lines. This moment is considered to be positive when, for angles of attack greater than the stable angle of attack, it tends to rotate the canopy in the direction toward the stable position. It is considered negative when, for angles of attack less than the stable angle of attack, it tends to rotate the canopy toward the stable position. Thus a stable position will exist when the moment diminishes to zero and the derivative $\frac{\partial C_M}{\partial \alpha} > 0$, where C_M is the moment coefficient and α is the angle of attack.

3) Drop Testing Procedure

Drop testing of models is used to verify the results obtained in wind tunnel tests. A descent rate of approximately 10 ft/sec is used for the 24-inch nominal diameter models, corresponding to a Reynolds number of about 1.3×10^5. In drop tests the angle of attack is determined by comparing the horizontal distance traveled to the vertical distance of descent. With properly adjusted suspension lines, the directional stability was sufficient to provide a steady descent which in turn was satisfactory for this mode of glide angle judgment.

IV. ANALYSIS AND RESULTS

Before the results are discussed in detail, the following general remarks may be in order.

The significant characteristic of a gliding parachute is that it has an inherent ability to prefer a gliding motion over all other motion. Such a decelerator must exhibit a stable gliding condition, maintained by a restoring moment. It has been shown that this condition exists when $\frac{\partial C_M}{\partial \alpha} > 0$ and the normal force diminishes to zero.

It was also noted that in general the gliding parachutes in the wind tunnel assumed their stable position at which they remained quite steady. However, when drop tested, many model configurations descended along a spiral, which would indicate a certain lack of yaw stability or lack of symmetry in the model.

It was found difficult to maintain full canopy inflation on some model configurations, particularly at relatively high glide angles. It was noted that at the limiting glide angle, the front portion of the canopy buckled inward and thus prevented the development of any higher lift to drag ratio. Therefore, the experiments with rigid models would only be of an exploratory nature, because rigid models would operate at large angles of attack, while their fabric counterparts are affected by buckling at these high angles.

A. Rigid Models

Table 1 presents the results of the investigation with eight rigid models. These tests showed that several rigid canopy configurations would approach or fully develop twice as much lift as drag, but selected fabric models did not reach these values because of collapse of the leading edge at large angles of attack. The Reynolds number of these tests with rigid models was on the order of 1.75 to 3.0 x 10^5.

B. Fabric Models

Table 2 summarizes the results obtained from experiments

TABLE 1. SUMMARY OF RESULTS FOR RIGID PARACHUTE MODELS

	MODEL	DESCRIPTION	ANGLE OF ATTACK (o)	L/D
a		EXTENDED SKIRT CANOPY	OSCILLATING BETWEEN 15° - 60°	
b	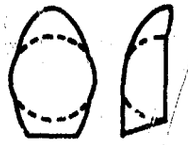	EXTENDED SKIRT CANOPY WITH TWO ATTACHED BODIES	35° ± 5°	0.70
c		10% EXTENDED SKIRT CANOPY	OSCILLATING BETWEEN 18° - 62°	
d		10% EXTENDED SKIRT CANOPY MODIFIED	64° ± 1°	2.05
e	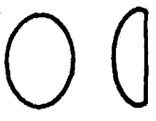	ELLIPTICAL CANOPY AXIS RATIO (1:1.65)	OSCILLATING BETWEEN 25° - 55°	
f		MODIFIED ELLIPTICAL CANOPY AXIS RATIO (1:1.65)	61° ± 1°	1.80
g		10% EXTENDED SKIRT CANOPY WITH GLIDING SURFACES	48° ± 3°	1.11
h		10% EXTENDED SKIRT CANOPY WITH GLIDING SURFACES SLOTTED	56° ± 3°	1.48

TABLE 2. TABULATED RESULTS FOR FABRIC PARACHUTE MODELS

Model	DESCRIPTION	POROSITY Ft^3/Ft^2-MIN.	Angle of ATTACK α	L/D	STABILITY	REMARKS
1	A 32" Nominal diameter unsymmetrical parachute. Shown in Fig 11.	120	$38^\circ \pm 3^\circ$	0.78	Completely Unstable	Inflation not maintained at large angles of attack because leading edge buckled.
2	A gliding parachute modified from a 37.5" diameter 10% extended skirt canopy. Shown in Fig 14.	120	$25^\circ \pm 3^\circ$	0.47	Stable	Fairly stable configuration but leading edge will buckle at an angle of attack of 30°.
3	A 16" nominal diameter parachute. Similar to model 2. Shown in Fig 16.	120	$22^\circ \pm 3^\circ$	0.40	Moderate Stability	This model tested on three component balance to obtain C_M, C_N, and C_T curves.
4	Modified 12" diameter ribbed guide surface parachute. Shown in Fig 17.	30	$40^\circ \pm 3^\circ$	0.84	Pitch $\pm 3^\circ$ Roll $\pm 5^\circ$ Yaw $\pm 5^\circ$	Very stable configuration. Used to develope method to keep canopy from collapsing.
5	16" nominal diameter gliding parachute having longitudinal ribs to support the canopy. Shown in Fig 18.	0	$57^\circ \pm 3^\circ$	1.55	Pitch $\pm 10^\circ$ Roll $\pm 40^\circ$ Yaw $\pm 15^\circ$	Very high α in wind tunnel but found to be unstable in drop tests.
6	24" nominal diameter gliding parachute having longitudinal ribs to support the canopy. Shown in Fig 19.	30	$50^\circ \pm 3^\circ$	1.19	Pitch $\pm 10^\circ$ Roll $\pm 30^\circ$ Yaw $\pm 10^\circ$	Higher porosity nylon help to stabilize this model but still "coned" in drop tests.
7	24" nominal diameter PARAFOIL GLIDER with slanted rib construction to support the canopy. Shown in Fig 20.	10	$48^\circ \pm 3^\circ$	1.10	Pitch $\pm 5^\circ$ Roll $\pm 10^\circ$ Yaw $\pm 5^\circ$	Stable configuration. Front of canopy will buckle at about $\alpha = 52^\circ$.
8	10 Foot nominal diameter prototype of model 7. Shown in Fig 22.	10	$50^\circ \pm 5^\circ$	1.19	Pitch $\pm 5^\circ$ Roll $\pm 10^\circ$ Yaw $\pm 5^\circ$	Appeared to be more stable than the smaller models. Good canopy inflation.
9	16" nominal diameter three component model of model 7. Shown in Fig 23.	10	$48^\circ \pm 3^\circ$	1.10	Pitch $\pm 5^\circ$ Roll $\pm 10^\circ$ Yaw $\pm 5^\circ$	Used to obtain C_M, C_N, and C_T curves in three component tests.
10	36" nominal diameter PARAFOIL GLIDER having 32 suspension lines. Shown in Fig 24.	10	$50^\circ \pm 3^\circ$	1.19	Pitch $\pm 5^\circ$ Roll $\pm 10^\circ$ Yaw $\pm 5^\circ$	This model was constructed to solve some structural problems.

with the fabric models. It can be seen that glide angles on the order of 50°, corresponding to a lift to drag ratio of 1.2, were reached.

Models 1, 2, and 3 represent the initial attempts to modify existing parachutes with unsymmetrical afterbodies. The main problem with these configurations was that of leading edge collapse. None of these parachutes reached an L/D of 0.5 and remained stable and inflated.

Models 4 through 10 evolved as an attempt to counter the problems found with the previous models. A description of the development of Models 4 through 7 is given in the Appendix. Table 2 shows that Model 5 achieved a stable angle of attack of 57° $\pm$ 3° or a lift to drag ratio of 1.55, but it was found in drop tests that the configuration of Model 5 was too unstable and cannot be recommended.

Modifications of Model 5 resulted in the configuration shown in Fig 24, represented by Models 7 through 10. It was found that these models had a stable angle of attack ranging up to 50° with an L/D ratio of 1.2.

It may be assumed that full size parachutes of the type represented by Model 10 will achieve a higher lift coefficient, based on experience with regular airfoils. Therefore, one may conclude that the lift to drag ratios obtained in these model tests are the lower limits of the respective lift to drag ratios.

C. Three Component Tests

Three of the configurations, namely, Models 3, 5, and 9, were tested on the three component balance. The results of these experiments are shown in Figs 29, 30, and 31.

Figure 29 shows the curves for Model 3, which is made of relatively high porosity cloth. It can be seen that this model has a stable angle of attack of 22° and the slope of the moment curve indicates a stable configuration. This model has a moderate tangent force coefficient of approximately 0.65 at its stable position.

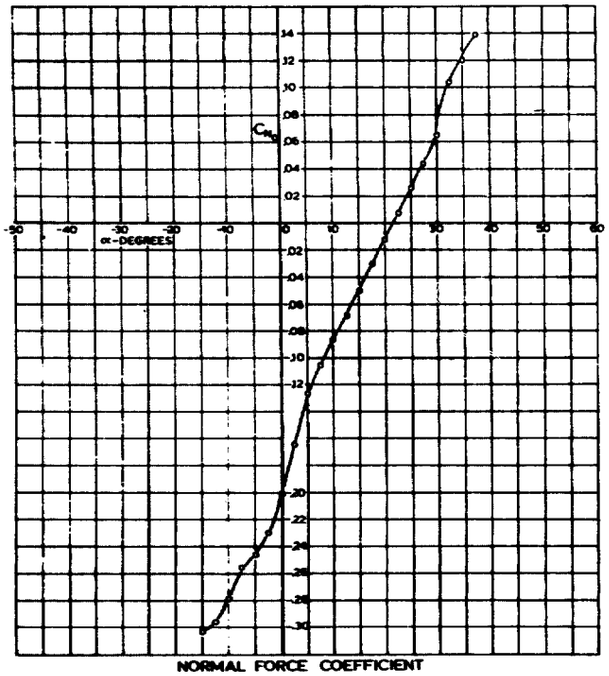

NORMAL FORCE COEFFICIENT

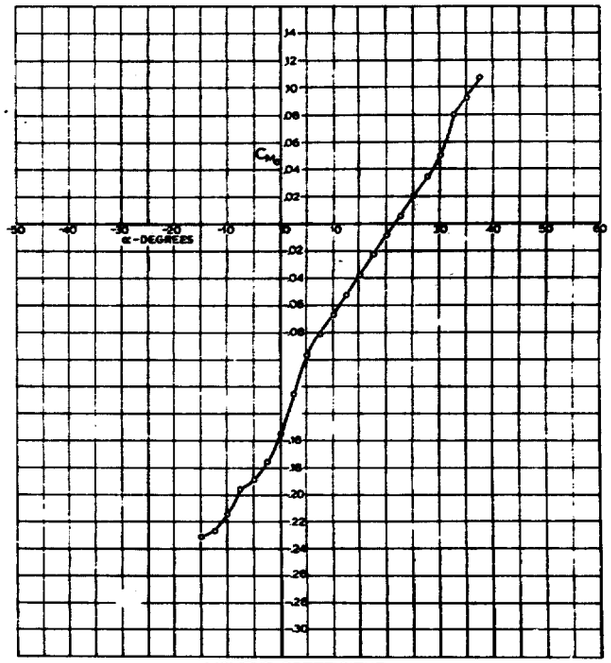

MOMENT COEFFICIENT

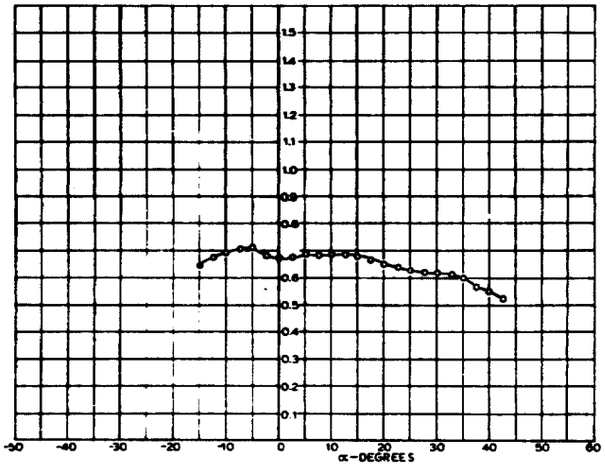

TANGENT FORCE COEFFICIENT

FIG 29. CHARACTERISTIC COEFFICIENTS vs. ANGLE OF ATTACK FOR MODEL-3, A GLIDING PARACHUTE MODIFIED FROM A 10% EXTENDED SKIRT CANOPY

BASED ON TOTAL SURFACE AREA S_o
REYNOLDS NUMBER = 5.6×10^5

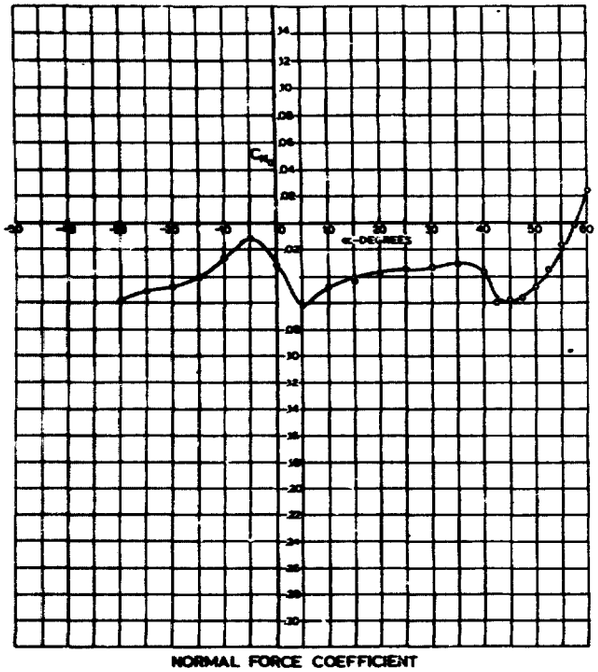

NORMAL FORCE COEFFICIENT

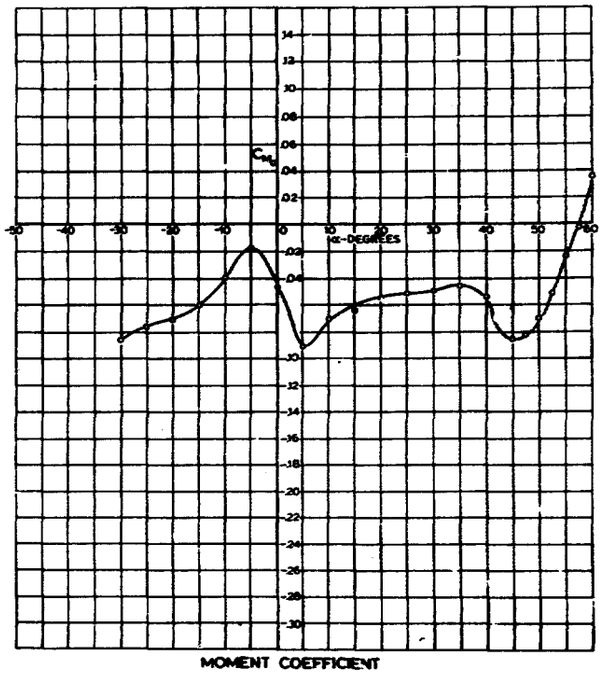

MOMENT COEFFICIENT

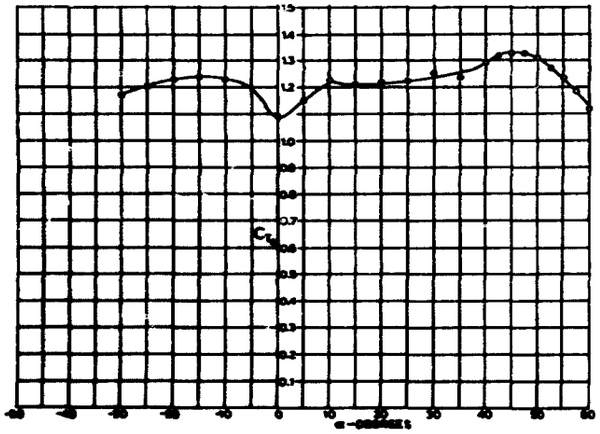

TANGENT FORCE COEFFICIENT

FIG 30. CHARACTERISTIC COEFFICIENTS vs. ANGLE OF ATTACK FOR MODEL-5, A GLIDING PARACHUTE CONSTRUCTED WITH ZERO POROSITY MYLAR COATED NYLON

BASED ON TOTAL SURFACE AREA S_o
REYNOLDS NUMBER = 5.6×10^5

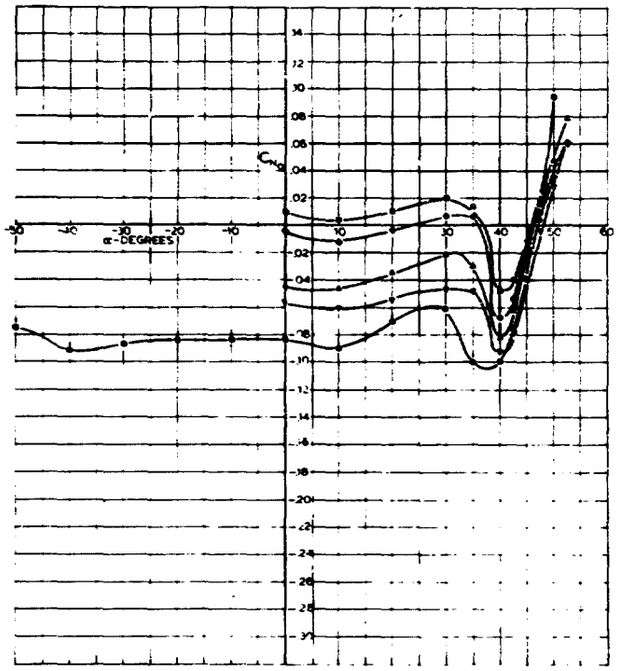

NORMAL FORCE COEFFICIENT

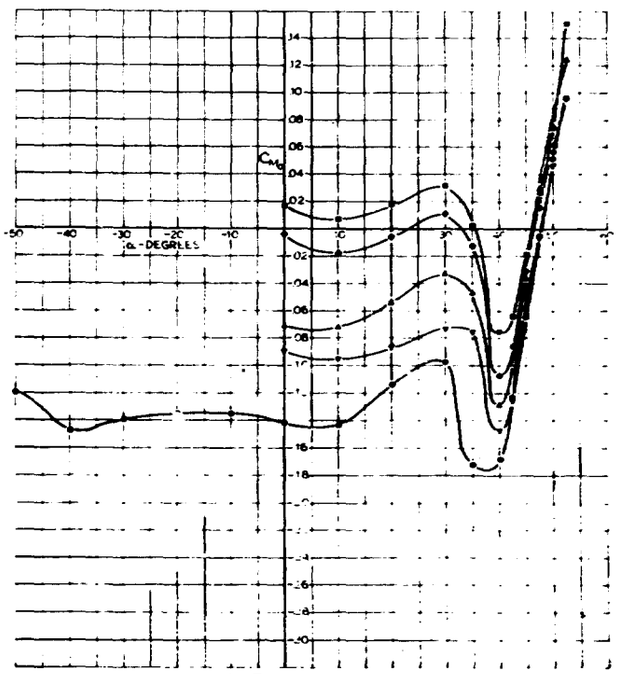

MOMENT COEFFICIENT

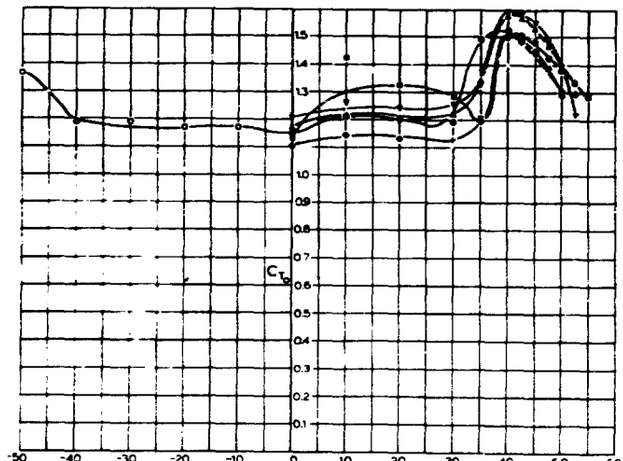

TANGENT FORCE COEFFICIENT

SYMBOL	RISER ADJUSTMENT $\delta = L_T - L_0$
●	0.050 D_0
▼	0.038 D_0
▲	0.025 D_0
◆	0.013 D_0
■	0.000 D_0

FIG 31. CHARACTERISTIC COEFFICIENTS vs. ANGLE OF ATTACK FOR A PARAFOIL GLIDER CONSTRUCTED WITH 10 POROSITY NYLON AT VARIOUS LINE ADJUSTMENTS.

BASED ON TOTAL SURFACE AREA S_0
REYNOLDS NUMBER = 5.0×10^5

Figure 30 shows the curves for Model 5. This zero porosity model exhibits a large stable angle of attack of 57° but the restoring moment is relatively weak and may not be sufficient to achieve satisfactory stability. This part is in agreement with the observations made in free drop tests.

The most successful configuration, Model 9, has its characteristic curves shown in Fig 31 for various line length adjustments. It can be seen that they are of the same general shape as those for Model 5, but have a lower stable angle of attack. However, it has a noted increase in stabilizing moment resulting in a more stable configuration.

The tangent force curve for this model reaches a maximum near the stable position. Hence, unlike Model 3 in Fig 29, the lift and drag of Model 9 increases near the stable angle of attack, thus creating a high tangent force. The maximum C_T value for this model is approximately 1.4 and would provide a relatively low rate of descent.

V. SUMMARY AND CONCLUSIONS

In summary, it was found that several rigid models possessed large stable angles of attack. The fabric models were subject to collapse and instability and the maximum glide angle of flexible models was lower than those of the rigid models.

In addition, it was shown that the models which indicated relatively large angles of attack would not necessarily be sufficiently stable in the three directions. Thus a compromise was obtained with a canopy which has a glide angle of approximately 48° or a lift to drag ratio of approximately 1.1.

It appears that to achieve larger glide angles would require parachutes based on entirely new design principles or with rigid front portions, leading edge support, or other mechanical contrivances.

APPENDIX

DESIGN, DEVELOPMENT, AND MODIFICATION OF THE PARAFOIL GLIDER

This section contains a description of the evolution of a gliding aerodynamic decelerator.

In designing a gliding parachute capable of operating at high angles of attack, the problems encountered in earlier designs, where canopy collapse was a prime performance factor, were carefully considered. To design a canopy which would present a thin leading edge to the flow, it was proposed that ribs be allowed to support the roof of the parachute. As a preliminary investigation of this type of design, a ribbed guide surface parachute was tested and modified.

The modified model, shown in Fig 17 of the main text, was obtained by removing portions of the guide surface panels at diametrically opposite sides of the canopy. This formed a channel through the canopy which allowed flow to pass without affecting the canopy skirt, that is, without causing buckling at the canopy skirt. When the suspension lines were properly adjusted, the modified portions would become the front and rear of the canopy in the flow. Upon completion of testing, this configuration displayed a stable angle of attack of $40° \pm 3°$ and was quite stable.

Since this model performed so well, a new configuration was designed which had ribs placed parallel to the flow, as shown in Fig 18. With this type of canopy the flow over the top of the canopy creates aerodynamic lift while the flow through the canopy reduces the drag. Since the roof panels are supported by ribs they may be constructed such that they are very nearly parallel to the flow and do not collapse.

Two parachutes were constructed with this design and subsequently tested; one of the models was constructed of 30 porosity nylon and the other of non-porous mylar. The model of zero porosity had a stable angle of attack of

57° ± 3°. The 30 porosity model was stable at an angle of attack of 50° ± 3°. These models are shown in Figs 18 and 19, respectively. It can be seen from Table 2 that these parachutes, listed as Models 5 and 6, were unstable and hence had to be modified.

To improve the characteristics of this design, modifications were made which produced a deeper canopy and one with slanted ribs. This configuration, shown in Fig 20, eventually attained an angle of attack of 48° ± 3°, which was less than the previous configuration but showed a marked improvement in stability.

Figure 21 shows the schematic drawing of the gliding parachute which was used in the following experiments and which has been referred to as the PARAFOIL GLIDER.

Since Model 7 (shown in Fig 20) was intended to be only an aerodynamic model, efforts were next directed at the development of a structural model. Two configurations were proposed and constructed. The first, Model 10 shown in Fig 24, had 32 suspension lines and 8 longitudinal ribs. This model achieved a stable angle of attack of 50° ± 3°, corresponding to an L/D of 1.20. Upon completion of testing, it was decided that 32 suspension lines were not necessary or desirable; consequently the model shown in Figs 32 and 33 was designed which had 24 suspension lines and 6 ribs.

Exploratory drop tests and wind tunnel tests of this cloth model with porosity of 10 ft^3/ft^2-min showed that it also had an L/D ratio of approximately 1.20. A schematic layout of the gores for this configuration is presented in Fig 34. Figures 35 through 39 show the dimensionless gore pattern layouts.

The nominal diameter of the canopy is calculated from the total canopy area excluding the area of the ribs. Figures 40 and 41 show the suspension line arrangement and lengths, where all suspension line lengths are measured from the skirt of the main canopy to the connection links. It should be noted that the suspension lines are continuous

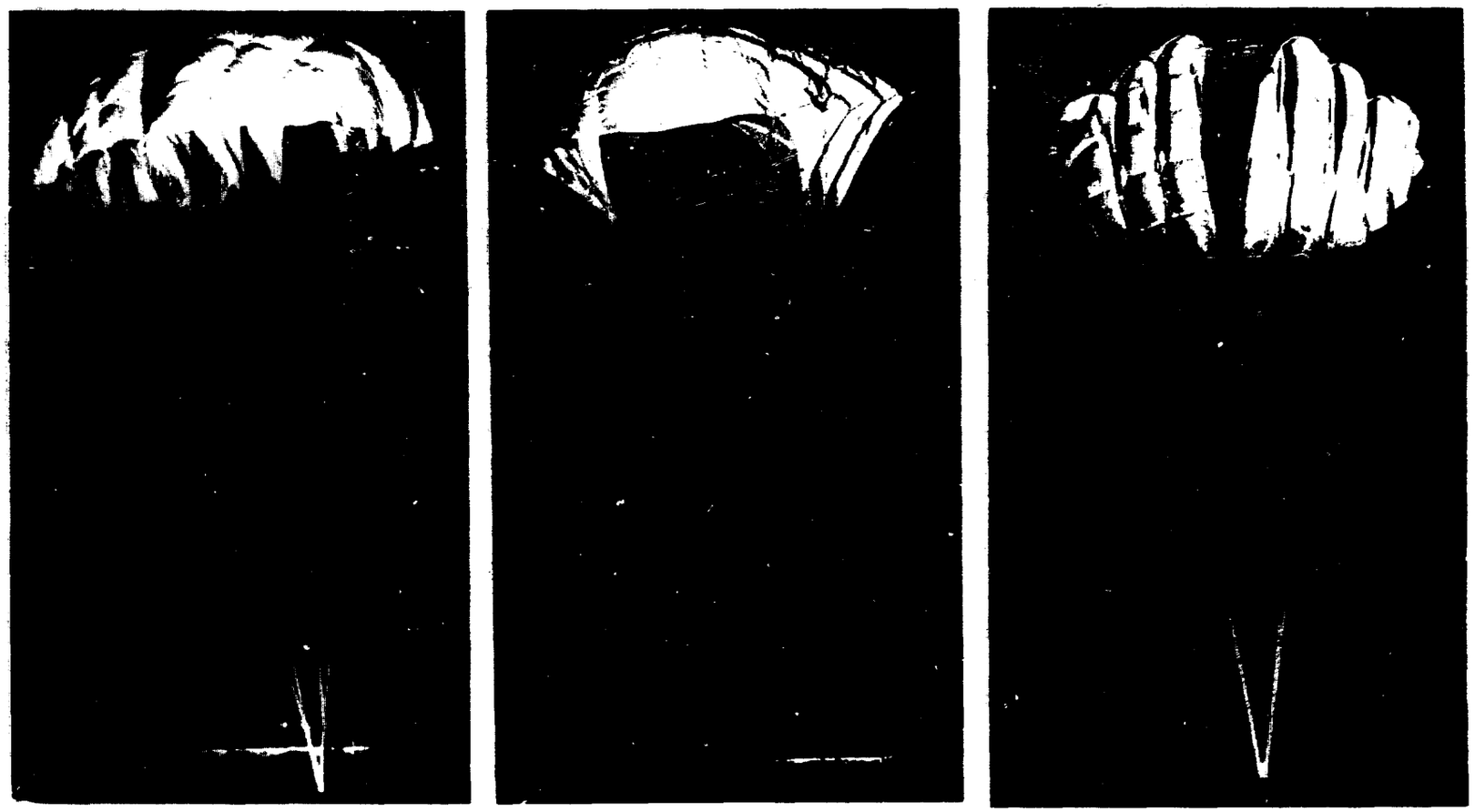

FIG. 32. PROFILE VIEWS OF 24 SUSPENSION LINE PARAFOIL GLIDER

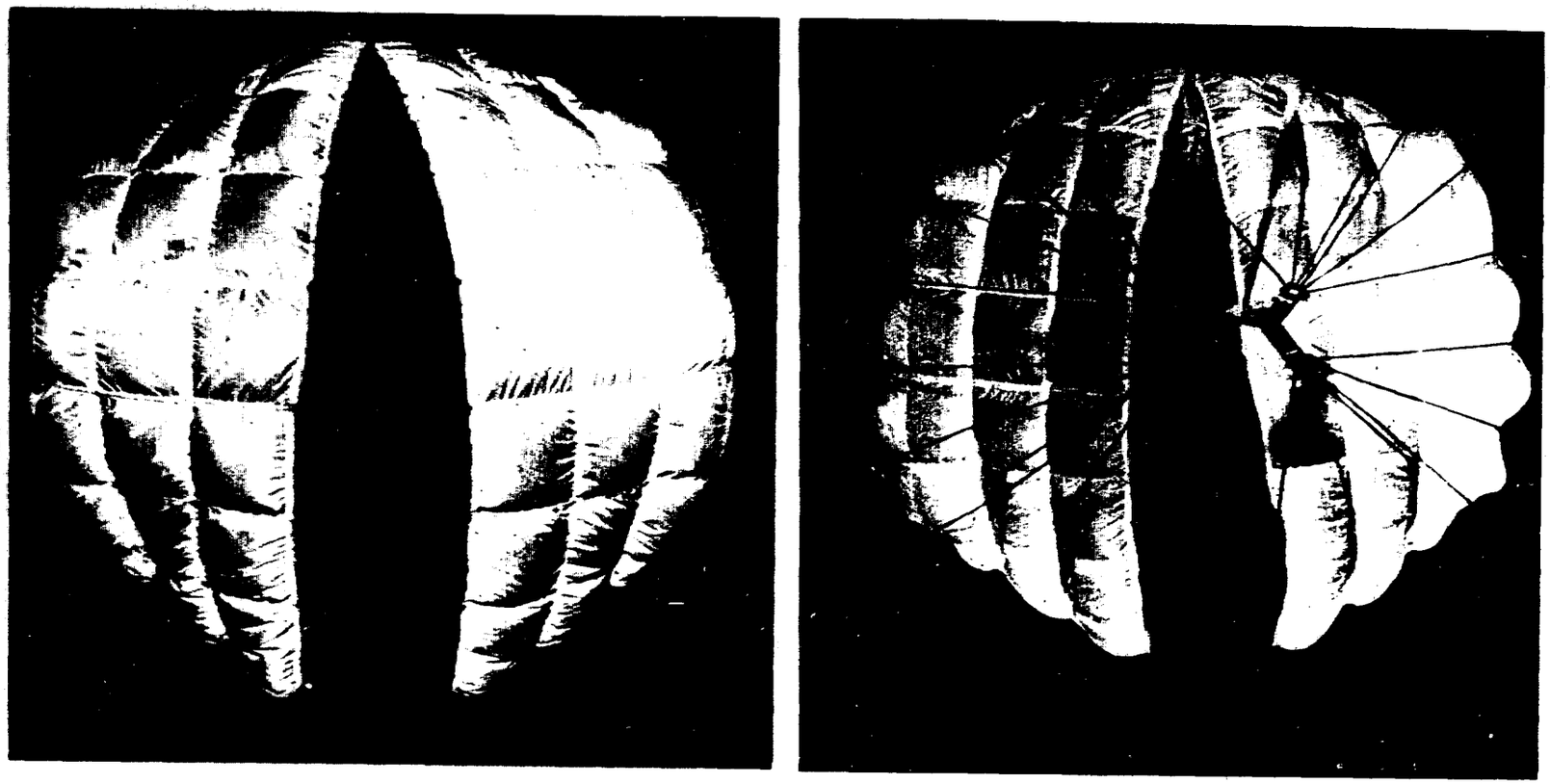

TOP VIEW

BOTTOM VIEW

FIG 33. INFLATED PARACHUTE CANOPY IN WIND TUNNEL
(24 SUSPENSION LINE MODEL)

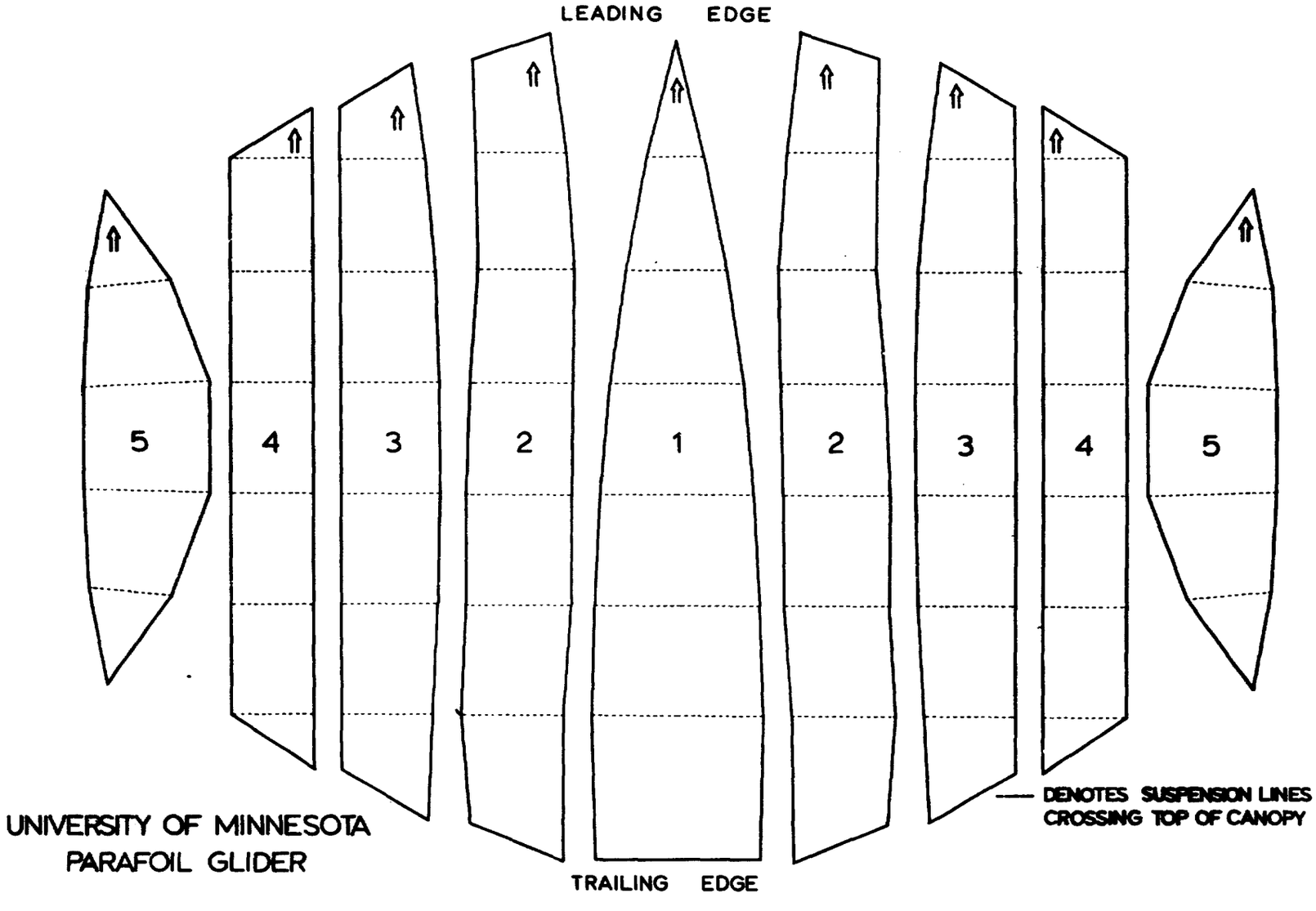

FIG 34. SCHEMATIC VIEW OF INDIVIDUAL GORES

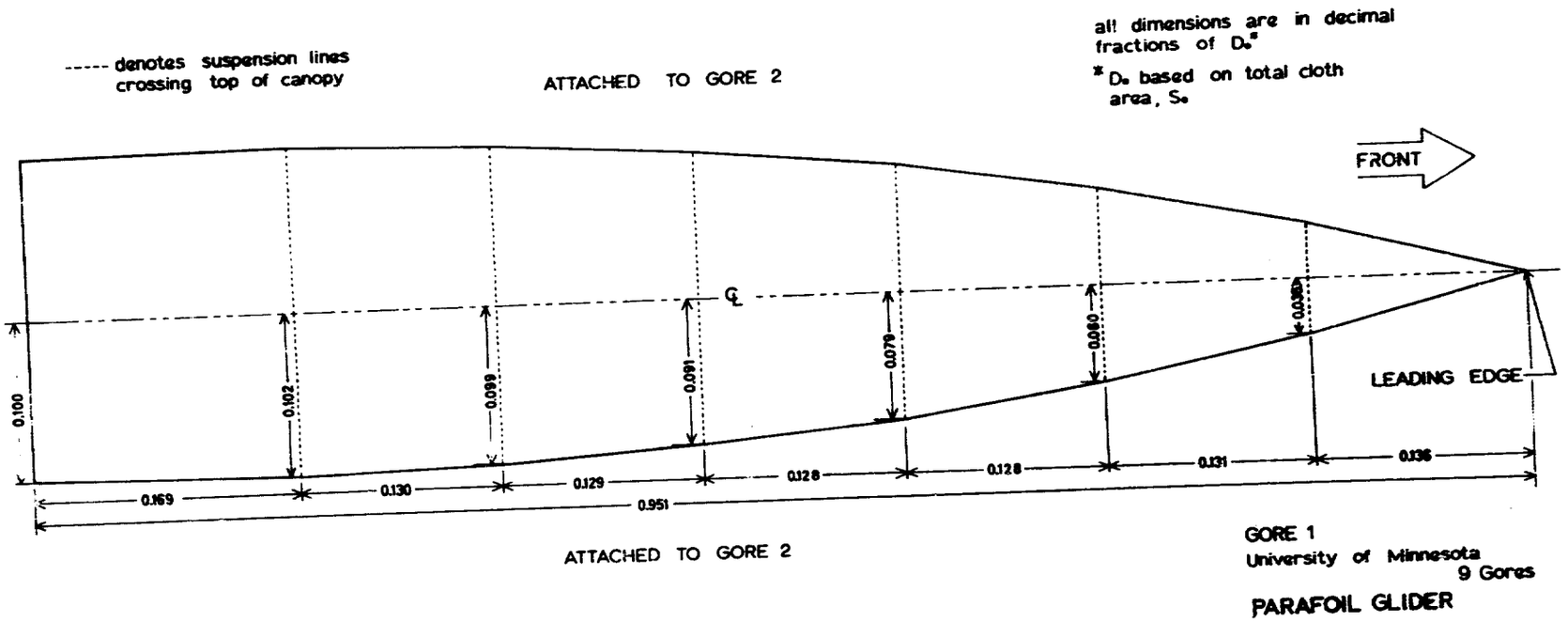

FIG 35. DIMENSIONLESS PATTERN FOR GORE NO. 1

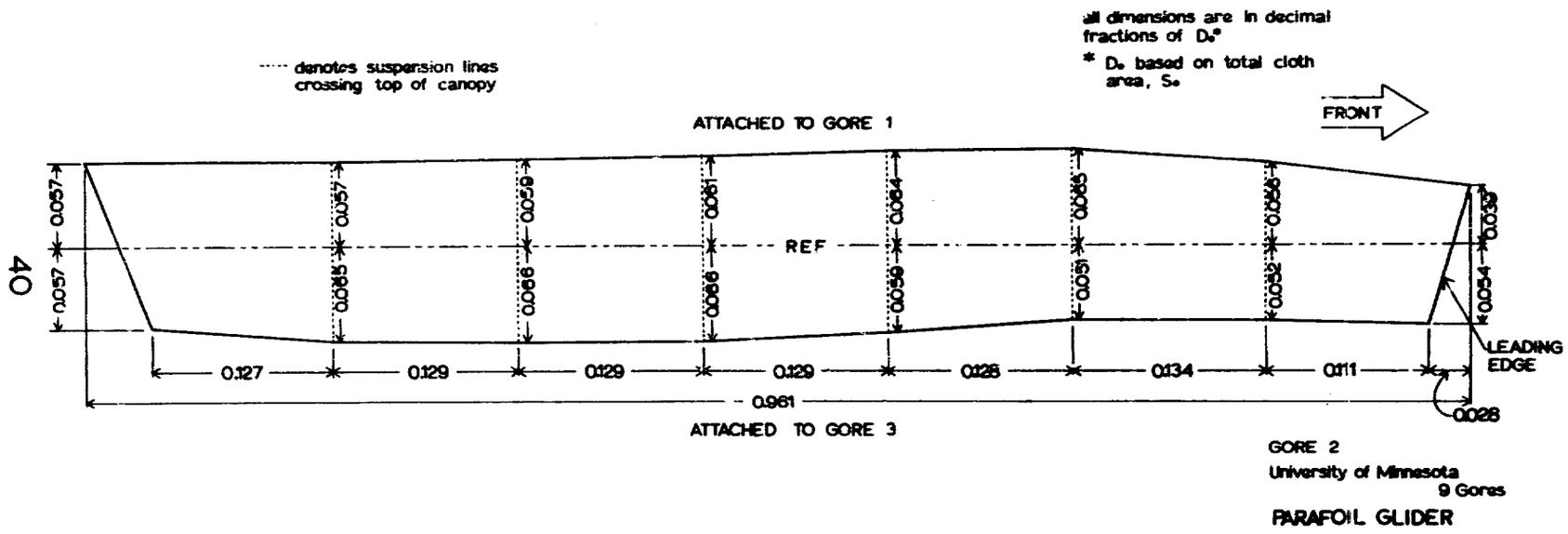

FIG 36. DIMENSIONLESS PATTERN FOR GORE NO. 2

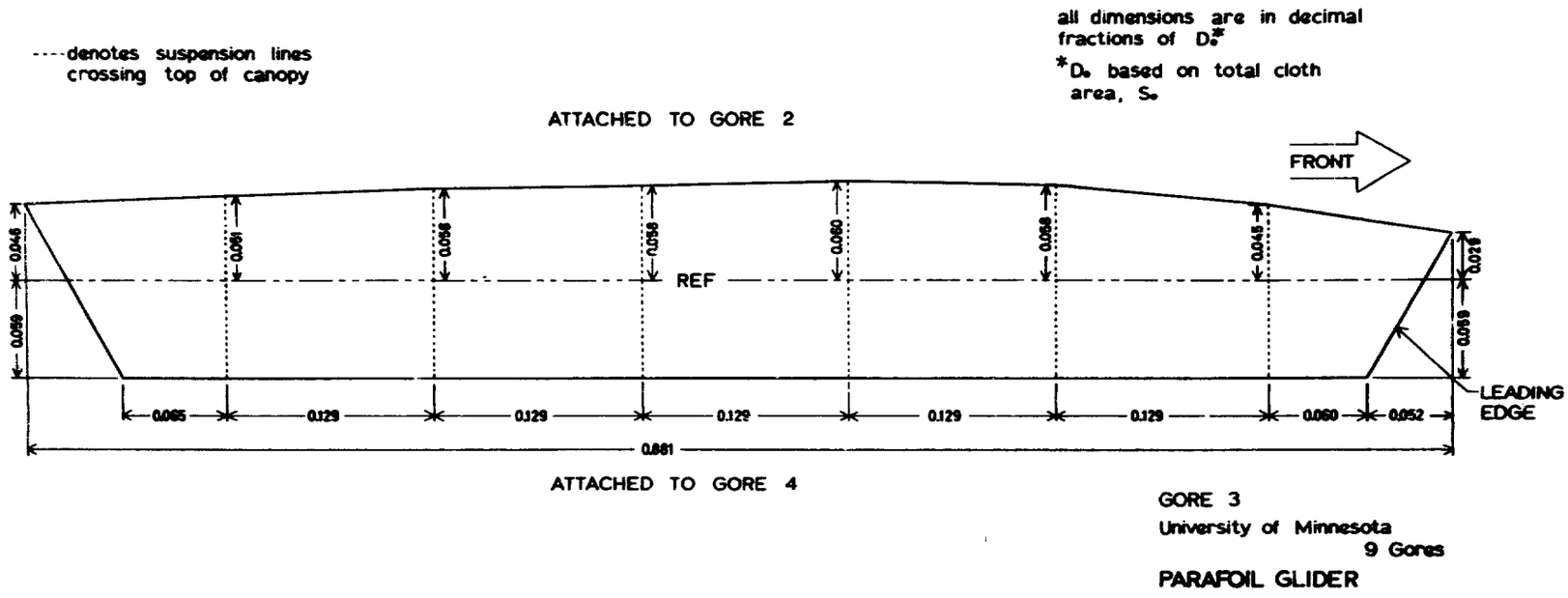

FIG 37. DIMENSIONLESS PATTERN FOR GORE NO. 3

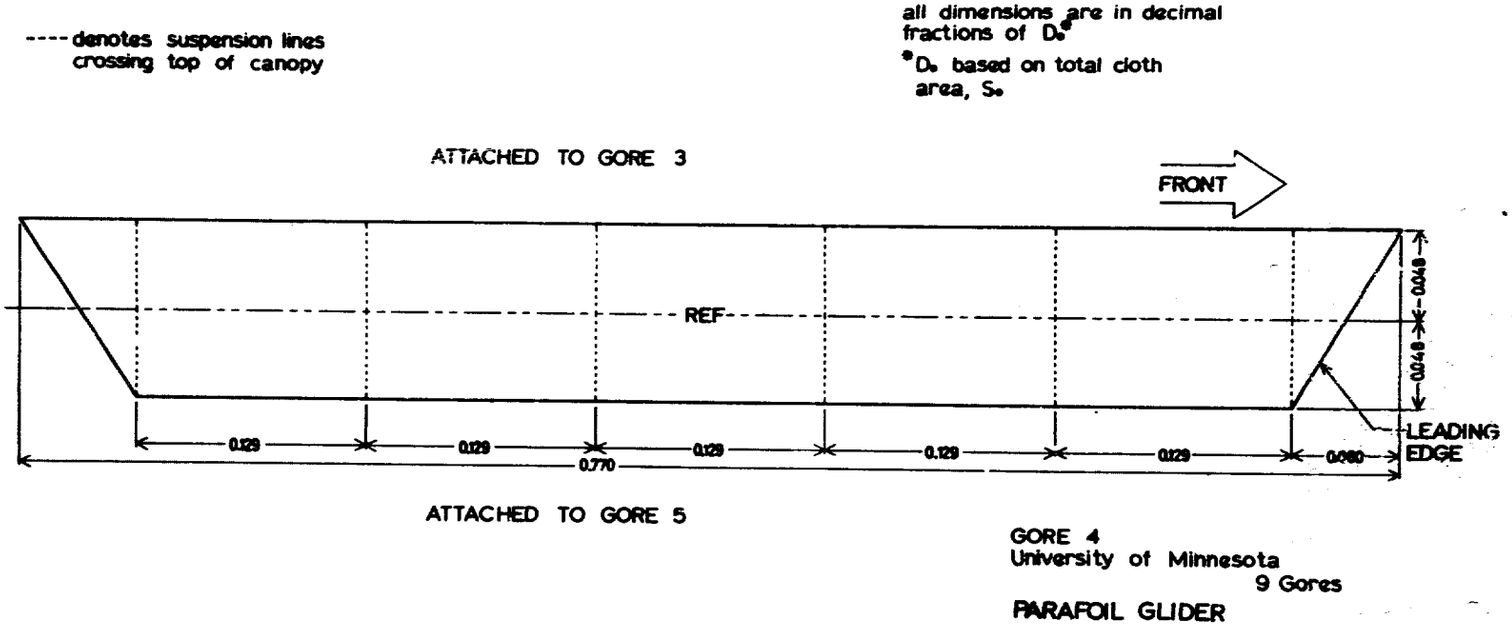

FIG 38. DIMENSIONLESS PATTERN FOR GORE NO. 4

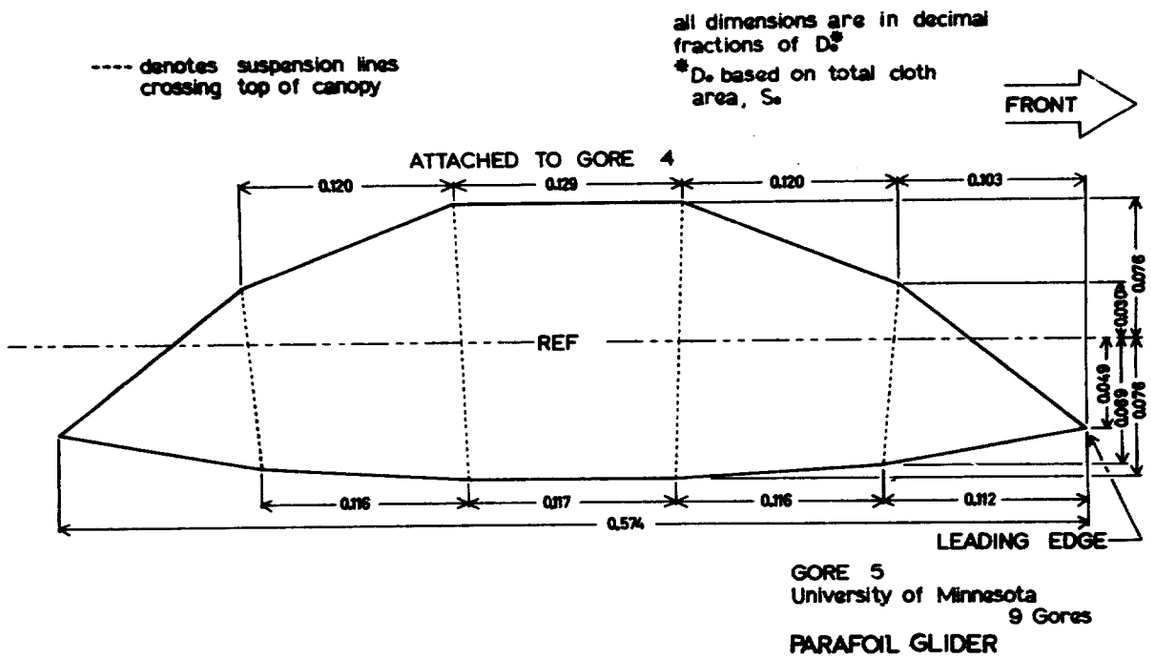

FIG 39. DIMENSIONLESS PATTERN FOR GORE NO. 5

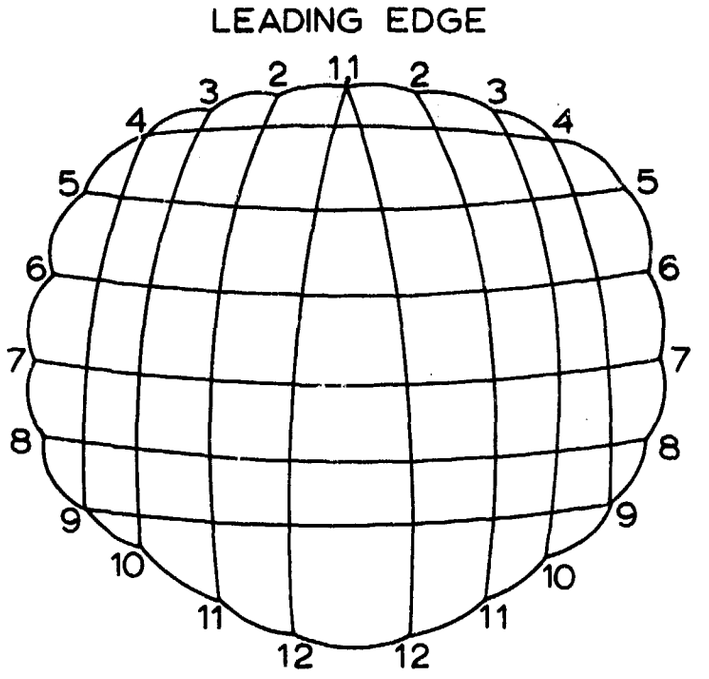

LINE NO	$\frac{\ell}{D_o}$	LINE NO	$\frac{\ell}{D_o}$
1	1.125	7	1.044
2	1.125	8	1.038
3	1.100	9	1.050
4	1.075	10	1.075
5	1.070	11	1.100
6	1.044	12	1.122

D_o based on total cloth area S_o

ℓ = length of suspension line measured from skirt of canopy to connection links on risers

Lines 1-6 on front risers

Lines 7-12 on back risers

FIG 40. SUSPENSION LINE LENGTH FOR 24-SUSPENSION LINE PARAFOIL GLIDER.

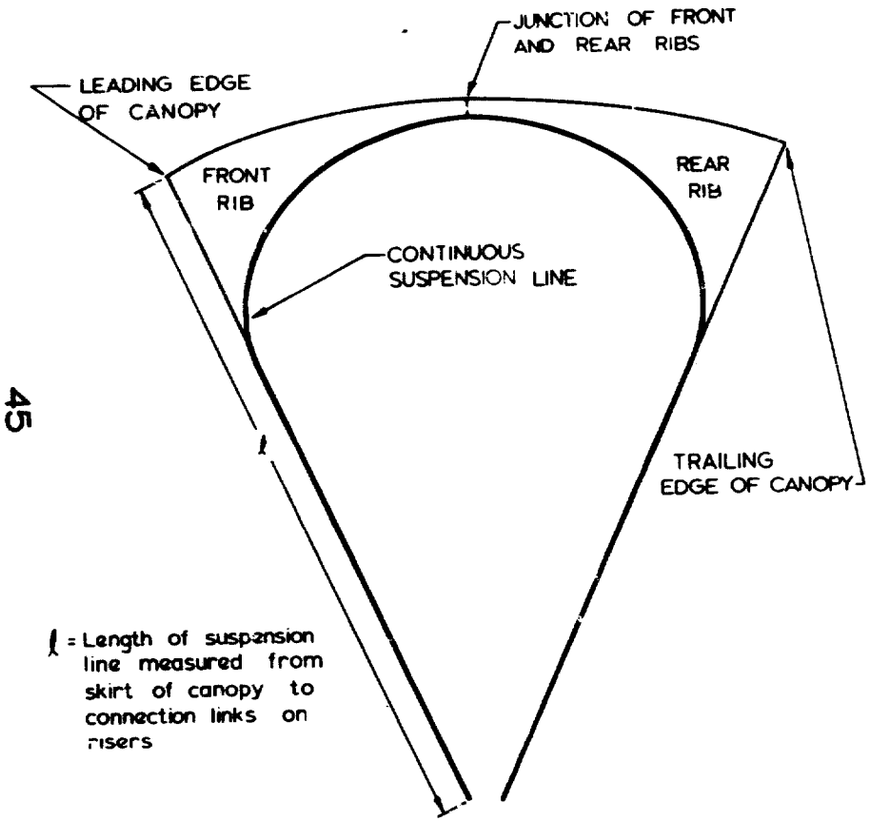

FIG 41. TYPICAL RIB PROFILE OF THE PARAFOIL GLIDER.

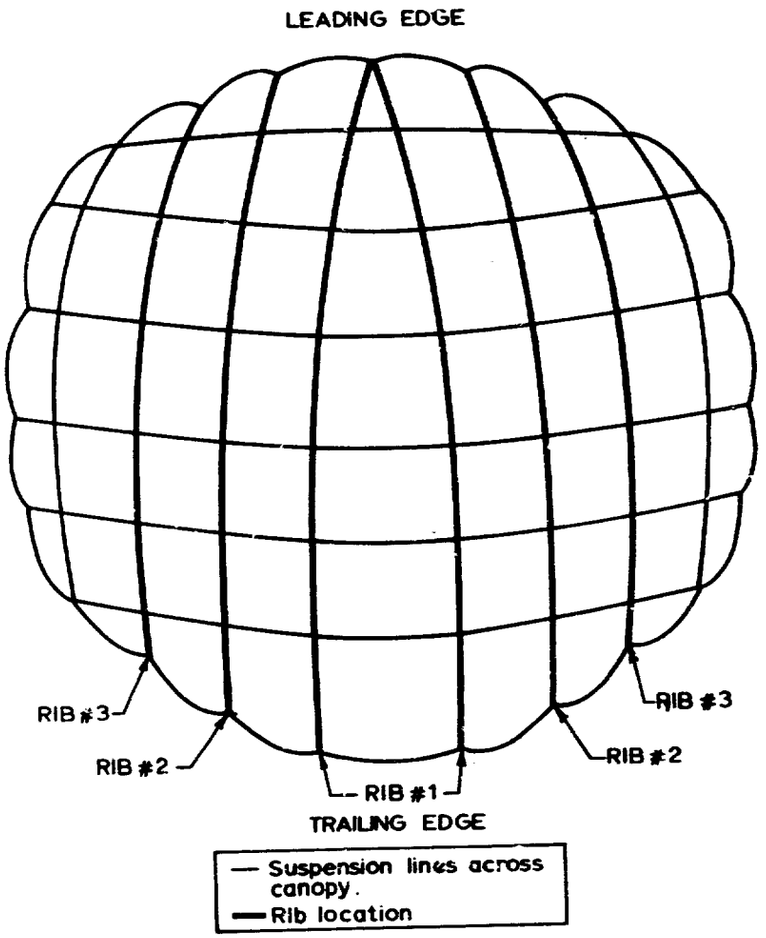

FIG 42. TOP VIEW OF INFLATED CANOPY PLANFORM AND RIB LOCATIONS.

across the bottom edge of the ribs. The risers used on this configuration were 0.15 D_o in length, thus increasing the over-all length of the suspension system to approximately 1.25 D_o.

A schematic view of the inflated canopy is shown in Fig 42 to indicate the location of the various ribs. The ribs themselves are attached along the seam of adjacent canopy panels. Figures 43 and 44 present the dimensionless gore patterns for the front and rear ribs. The shape of the front and rear ribs which are joined at the center of the canopy are nearly identical except for a slight difference on the top edge.

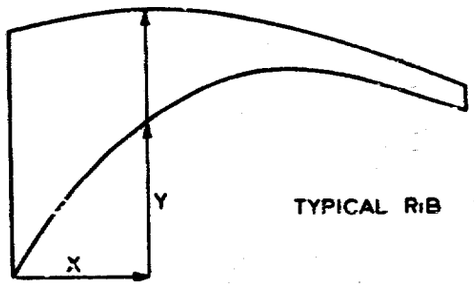

TYPICAL RIB

RIB #1

X/D₀	0	.05	.10	.15	.20	.25	.30	.35	.40	.45
Y/D₀	.244 .00	.246 .075	.243 .127	.234 .154	.217 .165	.198 .169	.174 .159	.150 .139	.125 .113	.091 .080

RIB #2

X/D₀	0	.05	.10	.15	.20	.25	.30	.35	.40	.45
Y/D₀	.206 0	.210 .064	.209 .120	.203 .140	.190 .145	.173 .145	.152 .135	.129 .116	.104 .093	.100 .078

RIB #3

X/D₀	0	.05	.10	.15	.20	.25	.30	.35	.40	
Y/D₀	.173 0	.176 .068	.176 .102	.173 .126	.165 .131	.153 .129	.138 .120	.120 .107	.105 .093	

FIG 43. DIMENSIONLESS GORE PATTERNS FOR FRONT RIBS OF PARAFOIL GLIDER.

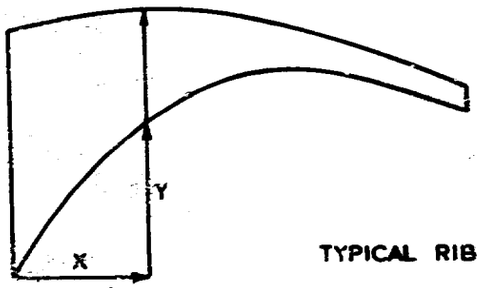

TYPICAL RIB

RIB #1

X/D₀	0	.05	.10	.15	.20	.25	.30	.35	.40	.45
Y/D₀	.272 0	.264 .075	.251 .127	.236 .154	.217 .165	.198 .169	.174 .159	.150 .139	.125 .113	.091 .080

RIB #2

X/D₀	0	.05	.10	.15	.20	.25	.30	.35	.40	.45
Y/D₀	.232 0	.223 .064	.214 .119	.203 .140	.190 .145	.173 .145	.152 .135	.129 .116	.104 .093	.100 .078

RIB #3

X/D₀	0	.05	.10	.15	.20	.25	.30	.35	.40	
Y/D₀	.195 0	.189 .068	.185 .102	.174 .126	.165 .131	.153 .129	.138 .120	.120 .107	.105 .093	

FIG 44. DIMENSIONLESS GORE PATTERNS FOR REAR RIBS OF PARAFOIL GLIDER.

REFERENCES

1. Heinrich, H. G. and Haak, E. L.: Stability and Drag of Parachutes With Varying Effective Porosity, ASD-TDR-62-100, December, 1961.

2. United States Air Force Parachute Handbook, WADC TR 55-265, December, 1956.

3. Heinrich, H. G., Haak, E. L., and Niccum, R. J.: Some Aerodynamic Characteristics of the RADIOPLANE GLIDESAIL Parachute and the ROGALLO PARAWING, sponsored by the Missile and Space Vehicle Department, General Electric Company, Philadelphia, Pennsylvania, January, 1962.